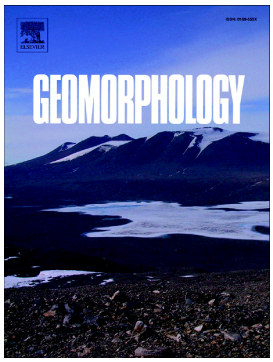

Tectonically driven drainage reorganization in the Eastern Cordillera, Colombia

Gaia Siravo, Paola Molin, Andrea Sembroni, Maria Giuditta Fellin, Claudio Faccenna

PII: S0169-555X(21)00255-5

DOI: https://doi.org/10.1016/j.geomorph.2021.107847

Reference: GEOMOR 107847

To appear in: *Geomorphology*

Received date: 31 October 2020

Revised date: 30 June 2021

Accepted date: 1 July 2021

Please cite this article as: G. Siravo, P. Molin, A. Sembroni, et al., Tectonically driven drainage reorganization in the Eastern Cordillera, Colombia, *Geomorphology* (2021), https://doi.org/10.1016/j.geomorph.2021.107847

Tectonically driven drainage reorganization in the Eastern Cordillera, Colombia

Gaia Siravo[1,2], Paola Molin[2], Andrea Sembroni[2,3], Maria Giuditta Fellin[4] and Claudio Faccenna[2, 5]

[1]Istituto Nazionale di Geofisica e Vulcanologia, Rome, Italy

[2]Dipartimento di Scienze, Università degli Studi Roma Tre, Roma, Italy

[3]Dipartimento di Beni Culturali, Università di Bologna, Bologna, Italy

[4]Department of Earth Sciences, ETH Zürich, Zürich, Switzerland

[5]Institute for Geophysics and Department of Geological Sciences, Jackson School of Geosciences, The University of Texas at Austin, Austin, TX, USA

Keywords: River capture; landscape evolution; active orogen; Colombia;

Corresponding author: Gaia Siravo (gaia.siravo@ingv.it)

Istituto Nazionale di Geofisica e Vulcanologia,

Via di Vigna Murata 605, 00143, Roma, Italy

Abstract

High-elevation plateaus that are positioned in between topographic barriers are common orogenic features in the South American continent, formed under a range of evolving environmental conditions. For example, in the central Andes (Bolivia-Argentina), the Puna-Altiplano is arid and endorheic with a poorly developed fluvial system, whilst in the northern Andes (Colombia) the Chiquinquirà and Tunja highlands are characterized by a humid equatorial exorheic fluvial system. In addition to a plateau-like low-relief surface at 2500 m, the landscape of the northern Eastern Cordillera and Santander Massif (northern Colombia) displays a lower elevation (~1500 m) low-relief landscape (Mesas) comprising river captures, windgaps, and a disconnected alluvial fan that collectively record a transient state. This configuration has been achieved through a combination of compressive deformation and sub-crustal processes. The compressive shortening started to occur in the Paleogene and is still active, whereas regional surface uplift related to slab flattening and mantle wedge hydration started in the Late Miocene/Pliocene. To disentangle the crustal vs sub-crustal forcing and to investigate the relative timing of drainage network evolution we combine the analysis of topography, hydrography (river longitudinal profiles, morphometric parameters, drainage divide stability), knickpoint migration (celerity model), paleo-longitudinal profile modelling, satellite images, and field observations.

In particular, we show that during the development of the low-relief Mesas landscape the older Chiquinquirà highland was a closed drainage and that the lower portion of the Suárez River flowed northward into the Bucaramanga depression forced by the Los Cobardes Anticline topographic barrier. The Suárez River collected waters from the southern Santander Massif and the upper reach of the Chicamocha River, which was draining the Tunja highland. An abandoned windgap deposit on the eastern edge of the Mesa de Barichara suggests that the lower portion of the Chicamocha River was not yet formed. Subsequent to the Chiquinquirà highland drainage opening, two main tributaries of the Magdalena River, the Lebrija and Sogamoso, captured the Suárez River in a short temporal sequence. A knickpoint celerity model allows us to date the Lebrija capture of the Bucaramanga depression at ~260-270 ka and the subsequent Sogamoso capture at 190-220 ka. Only during this final stage, the lowermost Chicamocha River section formed and the drainage network developed to its present configuration.

Finally, we suggest that the early Cenozoic rift inversion has controlled the drainage network pattern and the late Miocene sub-crustal-induced surface uplift has driven the main fluvial network reorganization.

1. Introduction

Orogens that form from either continent-continent or ocean-continent collision may develop high-elevation plateaus (e.g. the Tibetan, the Eastern Anatolian, the Puna-Altiplano). These plateaus can either be 1) internally drained or 2) externally drained, with the plateau margins dissected by deeply incised valleys. This regional-scale morphology often preserves deposits or landforms that record the integration of the fluvial network as the mountain chain builds and deforms. Indeed, uplift induces changes in base level, enhancing the potential energy (that increases stream power; Whipple and Tucker, 1999), sometimes resulting in the occurrence of river capture events that drive hydrographic reorganization. In the Central Andes, the Puna-Altiplano plateau is internally drained and stands at a mean elevation of more than 3000 m (Isacks, 1988, 1992; Kennan et al., 1997; Vandervoort et al., 1995; Barke and Lamb, 2006). Its drainage network evolved into an internally drained system due to uplift as a double-vergent orogen. This created an arid environment on its lee-side limiting erosion (see Strecker et al., 2007 for a review). Persistent arid conditions kept the intermontane plateau internally drained by preventing incision into the plateau margins by the regional drainage network (Sobel et al., 2003; Hilley and Strecker, 2005). A further example is the northern Andes and its Eastern Cordillera of Colombia where a plateau standing at ~2500 m is surrounded by 3000-5000 m high mountain ridges. Similar to the Puna-Altiplano, the ridges as topographic barriers made the plateau originally endorheic (Torres et al., 2005; Vriend et al., 2012), later changing to exhoreic as the regional drainage network integrated the plateau (Struth et al., 2017; 2020). If aridity facilitated the preservation of the Puna-Altiplano plateau inhibiting fluvial processes (Sobel et al., 2003; Hilley and Strecker, 2005), then the humidity of the equatorial climate of Colombia may have helped the opening of the endorheic plateau? However, is this the only factor that drove the hydrographic re-organization? Could the regional tectonics have contributed to the drainage integration of the plateau?

In the case of the Colombian Eastern Cordillera (EC), the landscape preserves a wide low-relief surface at an elevation of ~2500 m, composed of the Chiquinquirà and Tunja highlands to the north and the Bogotá highland to the south. Interpreted as an uplifted paleolandscape (Hooghiemstra et al., 2006), geologic evidence for the Bogotá and Chiquinquirà highlands suggests a formerly closed drainage basin (Torres et al., 2005; Vriend et al., 2012) that could have been similar to the modern Puna-Altiplano plateau in the central Andes (Caballero et al., 2013). Additionally, a complex drainage network comprising the Sogamoso and Lebrija drainage basins displays abandoned fluvial deposits, windgaps, deeply incised valleys, and river elbows (Julivert, 1958; Ingeominas 2008; Struth et al., 2020), collectively indicating a transient state and ongoing hydrographic reorganization. This could result from a post-Early-Pliocene base-level fall (Struth et al., 2020),

although this re-organization model only considers the highlands at ~2500 m as relict landscape surfaces. It disregards the low-relief surface (Mesas) positioned at ~1500 m which occupies a large portion of the EC, a surface previously interpreted as a Pliocene erosional landscape (Julivert, 1958). Moreover, the EC and its northward extension, the Santander Massif, is an active mountain belt with a complex tectonic evolution characterized by variable-scale geodynamic processes. The EC formed primarily by slow inversion of extensional faults initiated during early deformation stages in the Paleocene (Parra et al., 2012; Caballero et al., 2013) and with increasing exhumation rates since the middle/late Miocene (Mora et al., 2008; 2015; Siravo et al., 2018). The main faults active in the Quaternary (París et al., 2000; Ingeominas 2008; Siravo et al., 2020) have a strong morphologic expression suggesting they played an important role in the landscape evolution. Besides active tectonics, the concurrence of slab flattening and hydration of the mantle wedge below the EC (Siravo et al., 2019) has also contributed to surface uplift since the late Miocene (Hooghiemstra et al., 2006; Anderson et al., 2015). Thus, different forcing factors may control the landscape evolution, whose record in the drainage network and landscape of the EC has not been fully explored yet.

Crustal and sub-crustal processes have a direct influence on the Earth's topography, generating a disequilibrium that surface processes tend to balance by erosion, transport, and sedimentation. In convergent margins, when rock uplift outpaces erosion rates, a high elevated topography is likely to be formed (Pazzaglia and Brandon, 2001). The dominance of tectonics in the growth of a mountain belt stops when erosion compensates uplift. In general, an increase in erosion rate through time is expected to occur as soon as the hillslopes steepen in response to tectonics and orographic precipitation (Whipple, 2001). Thus, the hydrographic network records the signal of these external changes and conveys them throughout the system, controlling the hillslope processes that denude the surface (Whipple and Tucker, 1999; Whipple, 2004). In this respect, the shape of the longitudinal profiles of bedrock channels records potential (e.g., climatic and/or tectonic) variations as deviations away from a characteristic equilibrium shape. These can be evaluated by several morphometric parameters (Whipple, 2004; Wobus et al., 2006; Perron and Royden, 2013; Whipple et al., 2017). Similarly, the topography itself reflects the interactions between variable-scale tectonics and geomorphic processes (Beaumont et al., 2000; Hovius, 2000; Molin et al., 2004). Therefore, combined hydrographic and topographic metrics coupled with the study of landforms in the field are powerful tools to explore the driving processes of landscape evolution.

In this contribution, we take advantage of a remarkable preservation of a variety of landforms in the northern EC to provide new insights into the timing of events that shaped the landscape. We achieve this via topographic and hydrographic analysis coupled with a knickpoint celerity model

and paleo-longitudinal profile modeling. These results are then combined with fieldwork and satellite image data, allowing reconstruction of the northern EC and Santander Massif landscape evolution from the late Miocene to the present. We show that early-exhumed fault structures controlled the drainage geometry and that late Miocene-Pliocene surface uplift induced increasing incision, and thereafter the integration of part of the 2500 m plateau (Chiquinquirà highland) into the regional drainage system. The subsequent erosion shaped the Mesas paleolandscape and induced fluvial network reorganization with two subsequent River captures. The reconstruction of the complex history of the high-elevation plateau of the EC suggests that, despite the fundamental role of climate in controlling the efficiency of surface processes, the tectonic forcing is dominant in driving the integration of the regional hydrographic network into the plateau.

2. Geologic and geomorphologic background

The interaction of the South American, Caribbean, and Nazca plates controlled the evolution of the northern Andes and the formation of three different orographic ranges in Colombia (Fig. 1a). The easternmost range is the EC; occurring some 400 km from the Nazca trench and bounded by the Middle Magdalena Valley to the west and the Llanos Basin to the east (Fig. 1b). North of 6 °N, the EC strikes NNW-SSE for 300 km, from 6 °N southwards it trends NNE-SSW for 500 km (Fig. 1). The northern portion, the Santander Massif, is bound to the west by the regional scale transpressive Bucaramanga fault (Toro, 1990; Velandia and Bermudez, 2018; Siravo et al., 2020).

The EC is a double-vergent mountain belt formed by Cenozoic inversion of a Mesozoic rift (Cooper et al., 1995; Sarmiento-Rojas et al., 2006; Mora et al., 2008; Jiménez et al., 2014). The first tectonic compression occurred in the Maastrichtian-Paleocene (Bayona et al., 2020 and references therein). Inversion of the extensional faults started along the western side of the EC and migrated eastward through time (Parra et al., 2009; Bayona et al., 2013; Mora et al., 2015; Siravo et al., 2018). Regional structures such as the Los Cobardes and the Arcabuco anticlines started to exhume in the Paleocene (Parra et al., 2012; Caballero et al., 2013; Reyes-Harker et al., 2015). A change from marine to continental conditions was completed by the Early Cenozoic (Bayona et al., 2008; Reyes-Harker et al., 2015). Endorheic conditions were established in the EC from the Eocene and in the Middle Magdalena Valley in the Oligocene (Silva et al., 2013). Ongoing deformation and exhumation in the Oligocene resulted in an increase in deformation rates in the middle-late Miocene (Mora et al., 2015; Siravo et al., 2018). Such propagation of exhumation with faster rates occurred at the same time as the main surface uplift event in the EC (Mora et al., 2008; 2015). Palynology, paleo-flora assemblages, and geochemical analysis in the Bogotá highland and further north suggest a gradual increase in elevation from moderate elevations (~700 m) starting from ~7.6 Ma onward

(Hooghiemstra et al., 2006; Anderson et al., 2015). The concurrence of slab-flattening and hydration of a mantle wedge has been proposed as a mechanism for increasing uplift (Siravo et al., 2019).

The youngest sedimentary record belongs to Plio-Pleistocene fluvio-lacustrine deposits, which unconformably overlie the older succession and infill intermountain depressions such as the Bogotá and Chiquinquirà highlands (van der Hammen, 1974; van der Hammen and Hooghiemstra, 2003; Torres et al., 2005; Vriend et al., 2012). Finally, the reopening of the Middle Magdalena basin in the Early Pliocene induced a drainage reorganization (Struth et al., 2020).

2.1 Main structures

In the EC, the main faults define blocks that display different landscape aspects (see section 2.2). For instance, the Santander Massif (max. elevation of ~4000 m a.s.l.) is bound to the west by the left-lateral transpressional Bucaramanga fault. The fault strikes NNW-SSE (Fig. 1; Toro, 1990; Velandia and Bermudez, 2018) and dips ~70° to the east (Siravo et al., 2020). The total horizontal displacement of the Bucaramanga fault is still debated (Campbell, 1965; Irving, 1971; Tschanz 1974; Boinet et al., 1989; Toro, 1990; Velandia and Bermudez, 2018) however, a displacement of 2.5 km has been proposed for the Plio-Pleistocene according to offset geomorphic features (Ingeominas, 2008; Jiménez et al., 2015; see section 2.2.2). Thermochronologic analysis on the central portion of the Santander Massif suggests exhumation from the late Eocene and during the entire Miocene, decreasing through time (Mora et al., 2015; van der Lelij et al., 2016; Amaya et al., 2017; Siravo et al., 2020). New thermochronologic data show that the southern portion of the Santander Massif underwent fast exhumation during the middle Miocene which continued at a steady rate during the Early Pliocene (Siravo et al., 2020). Additionally, paleo-seismologic studies infer the occurrences of 7-7.4 Ms earthquakes with a recurrence of 1000 yr during the Holocene (Diederix et al., 2009), although, no seismicity is recorded during historic time.

To the south of the Santander Massif, the fault splits into two inverted high-angle thrust faults: the Boyacá and Soapaga faults (Toro, 1990; Fig. 1c). The hangingwall area of the Boyacá and Soapaga faults is called the Floresta Massif (Fig. 1), which continues further west downslope to the Mesas landscape. The Floresta Massif comprises basement rocks, an early Mesozoic granitic intrusion, and Jurassic sedimentary rocks (Dörr et al., 1995; Cediel et al., 2003; Saylor et al., 2012; Fig. 1c). The Boyacá and Soapaga faults together with the Bucaramanga fault constitute a system that was possibly transtensional during the Mesozoic (Cooper et al., 1995; Kammer and Sánchez, 2006) changing to transpressional in the Cenozoic (Toro, 1990; Mora and García 2006). Their activity has

been linked to the Late Eocene-Early Oligocene and to the Early-Late Oligocene respectively (Saylor et al., 2012).

The Mesas are delimited to the west by the Suárez thrust fault. This is an Early Mesozoic extensional fault trending NNE-SSW dipping to the NNW (Fig. 1c). It extends from ~6° N northward, terminating against the Bucaramanga fault. In the hangingwall of the Suárez fault, the related Los Cobardes Anticline exposes the Jurassic syn-rift succession (Fig. 1c). These rocks are thrusted over the Upper Cretaceous succession and Quaternary deposits (Ingeominas, 2008). Thermochronologic analysis dates the exhumation of this anticline to between the Late Paleocene and middle Eocene (Caballero et al., 2013). The Suárez thrust displays left-lateral oblique displacement and is considered still active in the Quaternary (París et al., 2000; Ingeominas, 2008).

2.2. Hydrography and morphologic features from satellites and field observations

Here, we summarize the main hydrographic and morphologic features from previous works and integrate them with our satellite images and field observations, focusing on the two main drainage basins of the northern EC and Santander Massif.

The study area is characterized by an equatorial climate with azonal variations in temperature and precipitation (Hermelin, 2016). The highest mean annual rainfall is recorded in the eastern foothills (~6000 mm/yr). In contrast, the axial EC is characterized by lower precipitation rates with the lowest values in the area of Bogotá highland (~1000 mm/yr) and in the Chicamocha River (~1500 mm/yr), but higher values occur in the Suárez River basin (3000 mm/yr; Hijmans et al., 2005; see Fig. S1 in supporting information).

The drainage network of the northern EC is characterized by short (~100 km) rivers, draining the eastern flank and joining the Orinoco River, and longer (~500 km) rivers, draining the chain interior and the western flank and joining the Magdalena River Among the latter, the Lebrija River and Sogamoso River drain most of the northern EC and Santander Massif. In both basins, the main trunk rivers (Sogamoso and Lebrija Rivers) flow ~N-S, parallel to regional faults, and display abrupt elbows to the NW when they cross the Suárez thrust and Los Cobardes anticline (Figs. 1b, 2).

2.2.1 Lower and Upper Paleolandscapes

In both the Sogamoso and Lebrija basins remnants of a wide sub-horizontal Pliocene surface (Julivert, 1958) occur at elevations of ~1400-1600 m, generally referred to as Mesas (Figs. 1b, 2). These remnants appear as isolated mesas bounded by gorges that resulted from the incision of an originally continuous surface by the modern drainage network (Figs. 2a, 3b). The layering of the Cretaceous sedimentary succession controls their gentle dips to the NW (Fig. 2b) and their top

surface configuration. Anticline-syncline axes produce local surface undulations configuring the drainage system to a trellis pattern (Fig. 2). From north to south, they are called the Mesa de Ruitoque, Mesa de Los Santos, and Mesa de Barichara, collectively forming the "lower paleolandscape" (Fig. 2b).

The Chiquinquirà and Tunja highlands are low-relief surfaces positioned between 2800- 2500 m. Wide and flat alluvial valley bottoms constitute much of their area and gentle surface undulation is present along syncline-anticline axes (Figs. 1c, 2). The valleys are presently connected to the drainage system through major knickpoints at 2500 m. In the Chiquinquirà highland, the uppermost Suárez River reach feeds and drains Lake Fúquene (Fig. 3f). The highland is filled by Plio-Pleistocene lake deposits (van der Hammen, 1974; Sarmiento et al., 2008; Vriend et al., 2012), positioned between 60 m below and up to 20 m above the present water level (van der Hammen, 1974; Vriend et al., 2012), suggesting the presence of a former larger lake within an endorheic drainage basin. Colluvium within the narrowest section of the river valley (upstream of the Suárez River exit from the highplain) could have dammed the river (Sarmiento et al., 2008). However, at the colluvium site, we observed a group of landslides that have rounded crowns and bodies with the typical shape of rotational slides evolving into flows or pure flows (Fig. 3g). Given that a sudden mass-wasting event is more likely to cause a natural dam than the slow sedimentation of colluvium, we infer that the occurrence of these landslides could have dammed the Suárez River rather than the colluvium.

The Tunja Highland has a similar appearance, although characterized by scattered and smaller flat valley bottoms, it lacks evidence of former enodorheic conditions (Servicio Geológico Colombiano, 2015). Together, both highlands constitute a wide low surface that extends southward into the Bogotá highplain. Finally, the Bogotá highplain, formerly endorheic region (Torres et al., 2005), has been recently connected to the present-day drainage (e.g. Struth et al., 2020). Collectively they constitute the "upper paleolandscape" (Fig. 2b).

2.2.2 Lebrija River catchment and the Bucaramanga alluvial fan

The Lebrija River catchment comprises the western portion of the Santander Massif (bounded by the Bucaramanga fault) and the Suárez fault escarpment (known as Palonegro) (Fig. 2). The Bucaramanga and Suárez faults bound a roughly triangular-shaped low relief area (Bucaramanga depression) that comprises the Bucaramanga alluvial fan (described below) and the Mesa de Ruitoque (Figs. 2; 3a).

The Lebrija River originates from the confluence of the De Oro and Suratà Rivers (channels 15 and 16 in Fig. 2a, respectively), both with sources in the western part of the Santander Massif at

elevation > 4000 m. The Suratà River and adjacent tributaries flow directly into the Lebrija River after crossing the Bucaramanga fault. To the south, the De Oro River and adjacent tributaries flow down from the Santander Massif, cross the Bucaramanga fault, and continue westward, reaching the base of the Palonegro escarpment (Fig. 2a). Here, the De Oro River turns from ~E-W to ~N-S, parallel to the Suárez fault. To the north, it incises the distal part of the Bucaramanga alluvial fan until the confluence with the Suratà River (channel 16 in Fig. 2a). Finally, the Lebrija River leaves the EC incising a ~400 m deep gorge to the NW across the Palonegro escarpment and the Los Cobardes anticline (LCA in Fig. 1b), north of Bucaramanga city.

The Bucaramanga alluvial fan (Fig. 3a) occupies an area that is 10-15 km wide and ~10 km long in the northern part of the Bucaramanga depression (Fig. 3c). The deposits are grouped into the Bucaramanga Fm., which is generally considered as Plio-Pleistocene age (De Porta, 1959). Magnetostratigraphy suggests the Bucaramanga Fm. spans 3-0.8 Ma (Jiménez et al., 2015). The Bucaramanga Fm. presents a maximum thickness of ~300 m (eastern portion; Ingeominas, 2001) comprising four members: Organos, Finos, Gravoso, and Limos Rojos (Hubach, 1952; Julivert, 1963; Bueno and Solarte, 1994; Vargas and Niño, 1992). The Organos member is a sequence of conglomerates with intercalations of fine sandstones. The Finos Member consists of clays evolving upward into fine-grained sandstone beds. The Gravoso member is a matrix-supported unit of gravel-size clasts overlying the Finos Member grading upward into the Limos Rojos Member. This latter consists of argillaceous sandstones and conglomeratic sandstones, interbedded with siltstone layers. Its top is at a mean elevation of 900 m, ~100 m lower than the Mesas located just to the west. Although the morphology of the Bucaramanga fan is partially masked by the densely populated namesake city (Fig. 3a), from field observations and remote sensing data it is still possible to recognize a convex surface with the elevation increasing from west to east towards the apex (Fig. 3a, c). The apex is positioned in contact with the Bucaramanga fault at the toe of the Santander Massif (Ingeominas, 2001; Jiménez et al., 2015) and appears disconnected from any river valley such that the location of its source area is unclear. It is commonly assumed that the fan was fed by the nearest Suratà River valley, placed 2.5 km north of the apex (Fig. 3a; c), before its displacement by strike-slip activity along the Bucaramanga fault (Ingeominas, 2001; Jiménez et al., 2015). Older alluvial fan deposits south of the Mesa de Ruitoque would support this hypothesis implying different strike-slip events (Ingeominas 2001).

An alternative hypothesis for the Bucaramanga fan deposition considers the presence of two windgaps (Julivert, 1958; Struth et al., 2020) along the southern segment of the Lebrija River divide, one located close to the Bucaramanga fault and the other close to the Palonegro escarpment

(Fig. 3c). The fan would have been fed by a northward-flowing drainage passing through the windgaps (Julivert, 1958; García et al., 2015; Tesón et al., 2015; Struth et al., 2020).

The eastern windgap is a narrow saddle controlled by the Bucaramanga fault, where no deposits were found by us nor described by previous authors (Fig. 3c). In other words, there is no strong evidence that the eastern windgap morphology is fluvial in origin. However, a narrow elbow in the present-day Chicamocha River pattern, just south of the eastern windgap (Fig. 2), has been used to support this hypothesis (Struth et al., 2020). Conversely, the more pronounced western windgap is currently the source for a small and ephemeral river (La Gacha). It drains from 800 m elevation, terminating abruptly to the south with a ~600 m drop, connecting with the Sogamoso River valley, exactly at its NW bend (Fig. 3c). The windgap valley is 500 m deep (Figs. 3c, d) and is aligned with the present Suárez River valley to the south, both being controlled by the Suárez thrust fault (Fig. 2).

Along the La Gacha River valley, fluvial deposits are widespread. The southernmost exposed deposit (i.e. closest to the windgap) is ~25 m thick comprising alternating fluvial sands and gravels (Fig. 3e). From bottom to top, we observed horizontal layers of rounded pebbles with local sand lenses. The pebbles range in size from 1 to 10 cm. Sedimentary, schists, and igneous rocks are the sources, with the largest pebbles, usually made of quartz. Sandy bodies alternated with gravel layers constitute the middle part of the outcrop. The sandy bodies are delimited by undulating erosion surfaces. These are locally overlain by channels of different sizes and made of cross-laminated coarse sands and gravels. The uppermost part of the outcrop consists of clast-supported gravels dominated by rounded pebbles in a sandy matrix, locally interbedded with sandy lenses. This deposit, dated with cosmogenic nuclides to 409 ka (Struth et al., 2017; 2020), is unlikely to be part of the Bucaramanga alluvial fan due to its markedly younger age but, together with the windgap, it calls for a former wider drainage area (Julivert, 1958; García et al., 2015; Tesón et al., 2015; Struth et al., 2020). Finally, provenance analysis on the windgap sediments and the Bucaramanga alluvial fan deposits provided contrasting interpretations between the Santander Massif source and the disrupted northward drainage system (Solano 2016; Plata-Guerrero and Moreno-Ruiz, 2015).

2.2.3 Suárez and Chicamocha Rivers (Sogamoso drainage basin)

The Sogamoso River basin is confined to the east by the Cocuy Sierra (CS), to the west by the Los Cobardes anticline, to the south by the Bogotá highland (BH in Fig. 1b), and to the north by the Lebrija River catchment (Figs. 1b, 2). The Sogamoso River forms at the confluence of the Suárez and Chicamocha Rivers, which converge at the southern toe of the Mesa de Los Santos (Fig. 2). The Suárez River sources in the Chiquinquirà highland (Figs. 2, 3f). Downstream of the highland, it

flows parallel to the Suárez fault and collects water from short western tributaries and long eastern tributaries, which incise the Mesa de Barichara. The uppermost tributaries incise the Arcabuco anticline close to its southern periclinal closure (Fig. 2), forming wide and deep antecedent valleys (Fig. 3h). However, a markedly reduced drainage area is present upstream of the anticline and no other rivers flow northward across the Arcabuco anticline and Floresta Massif, as these are topographic barriers.

The upper reach of the Chicamocha River meanders through the Tunja highlands. At ~2500 m, it exits the low relief area and flows northward following an arcuate pattern to the east of the Soapaga fault (Fig. 2). It collects water from both the Floresta Massif and the CS. Rivers draining the higher CS incise through Pleistocene glacial landforms (Fabre et al., 1982, 1985; van der Hammen, 1985; IDEAM, 2001). Downstream, it flows along the Bucaramanga fault trace for ~40 km after a major elbow to the NNW. Further downstream, the Chicamocha River turns to the SSW forming a second narrow elbow, passes in between the Barichara and de los Santos mesas, and finally merges with the Suárez River into the Sogamoso River (Fig. 2a). The Sogamoso River then flows over a short distance parallel to the Suárez fault and, similarly to the Lebrija River, exiting the EC via a sharp NW turn through a ~1000 m deep gorge incised across the Suárez fault and the Los Cobardes anticline (Fig. 2a). Low average erosion rates along the Chicamocha River basin have been linked partly to arid conditions in the lower Chicamocha valley (Struth et al., 2017).

3. Methods

To investigate the landscape evolution of the northern EC, we performed a morphometric analysis of the topography and drainage network of the study area. We used the Shuttle Radar Topography Mission (SRTM) Digital Elevation Model (DEM; ~90 m in horizontal resolution) as the elevation data source. Topographic maps (1:25000, Carta General; Instituto geográfico "Agustin Codazzi", 1998) have been used to check for local errors in the DEM and used to correct the elevation of some pixels.

3.1 Topography

The study area topography has been investigated by a slope map (Fig. 2), three swath profiles (Fig. 5), and a local relief map (Fig. 6).

The slope map is derived from the SRTM DEM to highlight the principal landforms, such as high-elevation plateau or steep escarpments. In order to identify low-relief areas, we focused the slope observation window on values lower than 30°. Therefore, we divided the slope map into 6 classes:

the first 5 classes characterize the landscape with slope angles lower than 30°; the last one marks the main scarps with slopes between 30° and 70° (Fig. 2).

Swath profiles were extracted using the Matlab TopoToolbox functions (Schwanghart and Kuhn, 2010), with a 20-km-wide observation window and sampling intervals of 500 m. The maximum and minimum topographies in the plot show the general configurations of the elevation peaks and valley bottoms, whereas the mean topography is representative of the regional scale pattern. In each swath profile, the local relief is calculated by subtracting the maximum and minimum elevation (Masek et al., 1994) (Fig. 5). This parameter allows quantification of river incision within the observation windows (Molin et al., 2004).

The local relief map provides insight into spatial variations of fluvial incision (Molin et al., 2004). It has been obtained by smoothing the maximum and minimum topographies with a circular window, 10 km in radius, and generating envelope and subenvelope surfaces. This value is chosen considering the mean valley spacing in the study area and allows the noisy influence of small valleys and ridges to be removed. The arithmetic subtraction of the subenvelope from the envelope results in the map of local relief (Molin et al., 2004).

3.2 Drainage network configuration

In tectonically active areas, the drainage network is considered to be one of the most sensitive indicators of uplift rate (Whipple, 2004). The EC offers a unique case to inform on plateau evolution as these landforms are now integrated into the drainage network. Additionally, the EC river network displays windgaps and elbows, suggesting an overall transient state. Nevertheless, the knowledge of the temporal sequence of the landscape shaping events is incomplete. Therefore, we performed a morphometric analysis of the drainage network using river longitudinal profiles, relative slope vs area analysis (Whipple, 2004; Wobus et al., 2006; Whipple et al., 2017), and drainage divide stability (Forte and Whipple, 2018). To explore the timing of the fluvial network organization as a consequence of river capture events, we run a knickpoint celerity model.

3.2.1 Stream longitudinal profiles and k_{sn} map

A stream longitudinal profile is a graph showing the variation in channel elevation versus its distance from source or outlet. When undisturbed longitudinal profiles have a typical smooth concave-up shape they are traditionally referred to as a graded, equilibrium profile, as described by the empirical Flint's equation (Mackin, 1948; Hack, 1973; Flint, 1974):

$$S = k_s A^{-\theta} \quad (1)$$

where S is the channel slope, A is the contributing drainage area, and k_s and θ are respectively the steepness and concavity indices. Deviations from this shape (knickpoints and knickzones) indicate that the fluvial system is in a transient state of disequilibrium in response to base-level change, or rock-type perturbation.

We extracted 17 longitudinal profiles from the main rivers and tributaries of the Sogamoso and Lebrija drainage basins using the Stream Profiler tool (Wobus et al., 2006). We focused on the area at elevations higher than 200 m because, at this elevation, the rivers leave the mountain relief and flow into the alluvial Middle Magdalena Basin. To quantify the shape of the longitudinal profiles, we calculated the values of concavity and steepness indices from the log-log S versus A plot. In detail, the k_s represents the y-intercept while the θ is the slope of a regression line through the slope and drainage area data. To allow a comparison of river longitudinal profiles, the values of the steepness index have been normalized (k_{sn}) to a theoretical value of concavity ($\theta_{ref} = 0.45$; Wobus et al., 2006 and references therein). This reference concavity derives from the empirical observation that, in steady-state longitudinal river profiles, θ varies from 0.35 and 0.65 (Wobus et al., 2006 and references therein).

Further analysis of the river long profiles was conducted using the χ plot of each river following Perron and Royden (2013). Here, a longitudinal profile is expressed as elevation vs a spatial integral of the drainage area (χ). This independent variable is expressed by the equation:

$$\chi = \int_{x_b}^{x} \left(\frac{A_0}{A(x)}\right)^{\frac{m}{n}} \quad (2)$$

Where x is the upstream distance and x_b is the outlet location, A is the drainage area and A_0 is a reference area, and m and n are constants whose ratio m/n is equivalent to θ in equation (1). This equation linearizes the river profiles, revealing possible knickpoints and allowing comparison between profiles. Note that in the χ plot the steepness index is the slope of a transformed river profile.

Finally, we extracted a map of the variation in k_{sn} along each studied channel (Fig. 8) using the automatic extraction tool of the Stream Profiler toolbar (Wobus et al., 2006). This allows direct observation of the spatial distribution of knickpoints and knickzones in the study area.

3.2.2 Drainage divide stability analysis

To investigate the drainage network evolution, we analyzed the stability of the divides between the Lebrija and Sogamoso Rivers and between the Suárez and Chicamocha Rivers. Drainage divide stability analysis allows for an evaluation of the influence of changes in river basin drainage area on the landscape evolution (Willet et al., 2014; Whipple et al., 2017, Forte and Whipple, 2018). The migration of a drainage divide was first studied by Gilbert (1877) who proposed that the asymmetry

on a divide means different erosion rates on either side. This difference causes the migration of the divide towards the side with a lower hillslope gradient and erosion rate. Perron and Royden (2013) and Willet et al. (2014) introduced a parameter termed χ, a proxy for steady-state channel elevation. Accordingly, where χ values are different across a divide, divide migration will occur with movement from lower to higher χ values until the anomaly is removed. Additional metrics (Gilbert metrics), calculated across the divide at a reference drainage area, have been proposed (Whipple et al., 2017) incorporating channel elevation, mean headwater hillslope gradient, and mean headwater local relief. Under conditions of non-uniform uplift rate, these parameters are more efficient than χ in defining the direction of divide migration (Whipple et al., 2017; Forte and Whipple, 2018). Indeed, whereas χ values are strictly dependent on rock erodibility and catchment outlet elevation, the Gilbert parameters are not (Forte and Whipple, 2018).

Drainage divide stability of the study area has been analyzed following Whipple et al. (2017) and using the MatLab Divide Tools (http://github.com/amforte/DivideTools) of Forte and Whipple (2018). This tool produces maps of Gilbert metrics and χ and compares the metrics in a plot where differences in the quantity of each parameter across the divide (delta values) are taken into account ("standardized delta plot" of Forte and Whipple, 2018). In this plot, a horizontal dashed line represents the divide stability condition. According to the divide orientation, the direction of migration is predicted when a point falls above or below this line. Considering the dependence of χ on outlet elevation, we produced a χ map by cropping the SRTM DEM to an elevation of 200 m, which approximates to the borders of the Eastern Cordillera, as well as being where the bedrock-alluvial channel transition occurs (see supplementary material at Figs. S2). We partitioned the divide into 9 sections, 25-30 km in length, following the geometry of the divide, and extracted the values of each parameter at a reference drainage area of 1 km^2. This value represents the critical threshold area downstream of which stream-flow-dominated channels are expected to dominate over debris-flow-dominated ones (Wobus et al., 2006). The numerical computation of χ has been performed by assuming 0.45 as the reference θ value. For each section, we represented the statistical distributions of the results of the four parameters in four histograms highlighting the mean value and the standard deviation (See supplementary material at Figs. S3-5). Finally, we elaborated the standardized delta plot (see supplementary material at Fig. S6) in order to compare the results relative to each metric (Fig. 9).

3.2.3 Knickpoint celerity model

In order to predict a time series of knickpoint positions in the Sogamoso River basin, we used a knickpoint celerity model following Berlin and Anderson (2007).

In the case of steady, uniform flow and detachment-limited conditions (sediment transport capacity exceeds sediment supply), the rate of bedrock river incision is considered equal to uplift rate and proportional to stream power (Howard and Kerby, 1983; Howard, 1994; Whipple and Tucker, 1999):

$$E = U = KA^m S^n \quad (3)$$

where *U* and *E* are, respectively, the rate of uplift and bedrock incision, *K* is a dimensional coefficient of erosion, *A* is drainage area, *S* is channel slope, and *m* and *n* are positive non-dimensional constants reflecting basin hydrology, hydraulic geometry, and erosion processes (Whipple and Tucker, 1999; Berlin and Anderson, 2007). The Sogamoso River drainage network is mostly characterized by bedrock or mixed bedrock-alluvial channels where the rock joints are related to tectonics and/or layering make plucking a dominant erosion process. For this reason, it is possible to consider Eq. (3) in the condition *n=1* (Whipple et al., 2000):

$$dz/dt = KA^m(dz/dx) \quad (4)$$

Rearranging *dz* we arrived at:

$$dx/dt = KA^m \quad (5)$$

where *dx/dt* is the upstream knickpoint migration rate in m/a. The formula defines the speed (or celerity) of a knickpoint propagating upstream and does not take into account changes in channel width or sediment flux, the effect of climate and the existence of an erosion threshold (Berlin and Anderson, 2007).

We modeled the propagation of two knickpoints found along the Suárez and Chicamocha Rivers at elevations of ~1000 and ~1520 m. In a capture scenario, the Suárez River flowed to the north including the present Lebrija River basin in its drainage area (Struth et al., 2020). After ~400 ka (Struth et al., 2020), the Sogamoso River was able to capture the Suárez River generating an erosion wave that disconnected the northern and southern portions of the basin and propagated upstream. The abandoned valley segment that connected the present Suarez and Lebrija basins became a windgap and part of the drainage divide. In this configuration, the point where the Sogamoso River meets the windgap (elevation 289 m) can be considered as an approximation of the capture site and the starting point of the erosion wave. We modeled the propagation of such a wave using a dynamic time-step approach (Crosby and Whipple, 2006; Berlin and Anderson, 2007), calculating the misfit by comparing the real knickpoints retreat distances with the predicted ones. *K* and *m* have been obtained by a forced search where the best fit is the combination of the two parameters that resulted in the lowest sum of squares of the misfit in the channels (e.g., Stock and Montgomery, 1999; Crosby and Whipple, 2006; Berlin and Anderson, 2007; Sembroni et al., 2016; 2020). The modeling requires a range for the K and m values. We fixed the K range at 10^{-7}-10^{-1} m^{1-2m} y^{-1} to

represent the whole range of lithologies outcropping in the study area (Stock and Montgomery, 1999; Whipple et al., 2000; Kirby and Whipple, 2001; Loget and Van Den Driessche, 2009; Giachetta et al., 2015; Sembroni et al., 2020). Given that θ is the ratio between m and n and that n can be fixed at 1 (Whipple and Tucker, 2002), θ is a good approximation of m (Giachetta et al., 2015) and it can be derived from the morphometric analysis (0–0.51; Table S1 in supporting information). The initiation time of knickpoint migration was modeled as starting sometime between 400 ka (which is the age of fluvial deposits outcropping near the windgap between the Lebrija and Sogamoso River basins; Struth et al., 2017; 2020) and present. We performed 100 simulations where each simulation is the best solution (lowest misfit) over 100,000 iterations. The results are shown in four histograms where the knickpoint starting age data are divided into 8 classes of 50 ka (see supplementary material at Fig. S7). Moreover, to have a unique time value for each model, we calculated the probability density functions (PDFs) for each histogram (Fig. 10).

To better constrain the results of the celerity model with the geometry of river longitudinal profiles and the windgap between Sogamoso and Lebrija Rivers close to the Palonegro escarpment, we reconstructed the shape of the former river profiles starting from segments of the Suárez and Chicamocha Rivers. To model these segments, we assumed that the portion of the river profile upstream of a knickpoint represents relics of a river under former equilibrium conditions (Gallen et al., 2013). In detail, we calculated the values of k_s and θ of each segment and, by a modified version of Eq. (1), we traced the paleo-longitudinal profile from a knickpoint towards the north, i.e. towards the windgap location. Assuming no significant tilting during the Quaternary, the elevation difference between the present and modeled profiles at the windgap could provide a minimum estimate of the incision (Kirby and Whipple, 2012; Gallen et al., 2013; Sembroni et al., 2020) that affected the area as a consequence of the capture of the Suárez River by the Sogamoso River

4. Results

4.1 Topography

The topography of the EC study area (Figs. 1b, 2) is characterized by slope values in the range 0°-70°, in contrast to the Magdalena and Llanos lowlands where slope values are always lower than 10°. In detail, in the central portion of the study area, several areas comprising slopes lower than 15° are located at different elevations in the Mesas (MB, MS, MR in Fig. 2) and in the highlands (CH and TH in Fig. 2). These low-relief areas are interrupted by the steep slopes (>30°) of fluvial valleys and/or tectonic structures (Fig. 2).

The northern swath profiles (Fig. 5a; for location see Fig. 1) show a strong asymmetry in the northern EC where ~5000 m of elevation difference occurs over 200 km along the western flank

(from the Middle Magdalena Valley up to the Cocuy Sierra top) and across <100 km along the eastern flank (from the Cocuy Sierra summit to the Llanos foreland; Fig. 5a). In the central portion of the mountain range, between the Los Cobardes Anticline and the Cocuy Sierra, the lower topography (~2000 m) of the Mesas gently decreases to the west. The Mesas are delimited by the incised valleys of the Suárez and Chicamocha Rivers. The drainage divide between these two main rivers runs along the hangingwall of the Boyacá fault (3000 m; Fig. 1). In the Los Cobardes Anticline and the Cocuy Sierra ranges, the drainage divide is offset relative to the highest elevations. In the Cocuy Sierra, the highest elevation of the minimum topography, the regional drainage divide between westward and eastward flowing Rivers of the EC, is to the west of the highest peaks. In the Los Cobardes Anticline, the divide between the Suárez River and the tributaries of the Magdalena River is located west of the highest maximum topography. Finally, the local relief shows a constant average value of ~1500 m throughout the chain with a minimum in the western portion of Mesa de Barichara (MB in Fig. 5a).

The swath profile b (Fig. 5b) shows a decrease in topographic asymmetry where the western flank is ~170 km wide, and the eastern flank <100 km. The highest peaks (less than 4000 m) are in the Cocuy Sierra. The regional divide between the Suárez River and the tributaries of the Magdalena River at the Los Cobardes anticline is slightly to the east of the highest maximum topography. In the central portion of the EC, the topography progressively increases from the Suárez River valley towards the Tunja highland. Here, the divide between the Suárez and Chicamocha drainages is located in the Boyacá fault-related highs (Fig. 1). To the east, the Tunja highland, where the Chicamocha River sources, is a low relief area whit an elevation of ~2500 m, characterized by alternating flat areas and ~200 m high ridges. The regional divide within the Cocuy Sierra coincides with the highest peak. In general, the maximum values of local relief (1500-2000 m) are found along the western flank of the Los Cobardes anticline and the eastern flank of Cocuy Sierra, where relief shifts from local topographic peaks towards the exterior of the chain. Lower local relief values are observed in the central portion of the EC, with a minimum within the Tunja highland.

The southernmost swath profile (Fig. 5c) shows the EC as an almost symmetric chain. The highest peaks of maximum topography stand at ~3500 m in the central portion of the chain, at a distance of <100 km from the foothills. The western and eastern regional divides are relatively close and located along the edges of the Chiquinquirà highland, where the source of the Suárez River and Lake Fúquene are located. As observed in swath profile b (Fig. 5b), the maximum local relief values (1500-2000 m) occur along the flanks of the chain and do not coincide with the local highest values of the maximum elevation. Similarly, the lowest values of local relief are found in the Chiquinquirà highland.

The local relief map (Fig. 6) shows average values higher than those extracted from the swath profiles but with a similar pattern. The local relief is generally higher on the flanks of the mountain range than in the central part. Here, the Chiquinquirà and Tunja highlands and the Mesas have local relief of < 500 m, whereas the Floresta Massif (FM in Fig. 6) shows values of > 1500 m. The entire Cocuy Sierra has generally high values that increase to the east. The map also shows that higher local relief values coincide with tectonic features (Fig. 6).

In summary, the topography of the EC changes progressively from asymmetric to symmetric from north to south. North of 6° N the chain is strongly asymmetric, with a high elevated peak off-centered to the east. To the south, the chain becomes progressively more and more symmetric with a high-standing low relief area in between two equally wide and steep flanks.

4.2 Drainage network configuration

4.2.1 Longitudinal profiles and χ plots

We extracted the longitudinal profiles of 17 main rivers draining the interior (i.e. rivers draining only flanks are excluded) of the northern EC and southern Santander Massif, an area encompassing the Sogamoso and Lebrija Rivers basins (Fig. 2). The longitudinal profiles and chi-plots are shown in Fig. 7. The main knickpoints are indicated on the geologic map of Fig. 1c. Along-stream θ and k_{sn} values are reported in Table S1 (supplementary materials).

The longitudinal profile of the Suárez River shows three pronounced knickpoints at 2500, 1450, and 1000 m of elevation, which result in a staircase-like profile (Fig. 7a). Upstream of the 2500 m knickpoint the upper reach of the Suárez River is more than 50 km long, almost flat, and coincides with the Chiquinquirà highland (including Lake Fúquene). An elevation drop of 1 km over only ~20 km distance occurs across the highest knickpoint. Along the upper reach, the channel is sinuous and alluvial but downstream of the 2500 m knickpoint, it becomes a bedrock channel characterized locally by a cascade or step and pool pattern. The Suarez River profile is approximately concave between the knickpoints at 2500 and 1450 m. It is composed of rectilinear segments between the knickpoints at 1450 and 1000 m. Downstream of the knickpoint at 1000 m, the profile is almost rectilinear. Here, the mixed alluvial-bedrock channel is characterized by a pool and riffle sequence up to the confluence with the Chicamocha River The χ plot of the Suárez River shows an upper segment (elevation >2500 m) shifted toward higher χ values and a lower one, much steeper and marked by the 1450 and 1000 m knickpoints.

The Suárez River drainage basin is asymmetric with very short (<tens of km) western tributaries that are not comparable with the other studied rivers (Fig. 2a), thus they are excluded from the analysis. The major tributaries feed the Suarez River from the Mesa de Barichara and the Floresta

Massif ridge (Fig. 2). Among the southern tributaries, channel 2 (Fig. 2a) has flat segments along a perched valley (syncline fold) at ~3330 m and along the Chiquinquirà highland (Figs. 2, 7a). Both channels 2 and 3 have a knickpoint at ~2000 m, across an anticline, and they flow into the Suárez River just before the major 1450 m knickpoint (Fig. 7a). The northern tributaries (channels 4 and 5) drain the Floresta Massif and the Mesa de Barichara and merge at a knickpoint at ~1100 m (Fig. 7a). The χ plots of the tributaries of the Suárez River (Fig. 7c) show a similar pattern interrupted by the several knickpoints described above. They are also significantly less steep than the Suárez River and with higher χ values.

The Chicamocha River profile has a concave smooth upper reach, with a meandering alluvial channel where it flows across the Tunja highland (Figs. 2 and 7a). This reach displays a knickpoint at 2500 m of elevation followed downstream by a ~50 km long convex knickzone with a cascade channel and an elevation drop of ~1 km. Downstream of the knickzone, the channel is braided and the river profile is rectilinear with some minor knickpoints (e.g. at 1500 and 1000 m). The χ plot (Fig. 7c) shows an almost rectilinear downstream segment and a net shift towards higher values along the upper reach.

The western tributaries (channels 7 and 8; Figs. 2, 7a) have longitudinal profiles with concave-up segments above 2500 and 3000 m (Fig. 7a), which coincide with small alluvial valleys located between the Soapaga and Boyacá thrusts (Fig. 2). The lower portion of their longitudinal profiles, characterized by a knickzone (~2300 m), comprises narrow valleys deeply incised into the bedrock, across the Soapaga fault. χ plots (Fig. 7c) show a shift towards higher values upstream of the 2500 and 3000 m knickpoints, and a generally rectilinear lower reach almost parallel to the downstream segment of the Chicamocha River. The northernmost western tributary (channel 9) is characterized by an upper concave-up reach (rectilinear in the χ plot) interrupted by the main knickpoint at ~1500 m and followed by a convex segment (shifted to lower values in the χ plot) down to the confluence with Chicamocha River (Figs. 7a, c).

The eastern tributaries of the Chicamocha River drain the 5000 m high Cocuy Sierra and the southern termination of the Santander Massif (Fig. 2). Whilst their upper reaches are characterized by several knickpoints and knickzones, the lower reaches are almost rectilinear (Fig. 7a). The knickpoints above ~3000 m (channels 10, 11, and 12) may be related to glacial landforms relative to Pleistocene glaciers (Fabre et al., 1981; 1985; van der Hammen, 1985; IDEAM, 2001). The χ plots of the eastern tributaries (Fig. 7c) are almost rectilinear and as steep as the downstream segment of the Chicamocha River plot.

In the Lebrija River catchment, the main De Oro River (channel 15) shows three pronounced bends that delimit four reaches: 1) a NE-SW high reach, draining the Santander Massif, 2) an E-W

reach between the Bucaramanga fault and the Suárez thrust, 3) a S-N low reach along the Suárez fault and, after joining the Lebrija River, 4) a NW-SE reach across the Suárez fault (Fig. 2). Similarly, the longitudinal profile is composed of a concave-up high reach (above 2000 m) and three rectilinear segments: 1) upstream of the Bucaramanga fault (between 2000 and ~900 m of elevation), 2) downstream of the Bucaramanga fault down to a knickpoint at ~600 m of elevation, and 3) downstream of the knickpoint (Fig. 7b). In the χ plot (Fig. 7d), similar reaches can be identified and the entire river profile displays a large shift towards higher χ values. Channel 17 shows an upper concave reach and a lower rectilinear segment, and on average shifts towards lower values in the χ plot. Channel 16 is composed of two rectilinear segments and its χ plot is substantially rectilinear. It is noteworthy that channels 16 and 17, and the upstream segment of channel 15 have a similar pattern to the eastern tributaries of the Chicamocha River, whereas the downstream reach of channel 15 resembles channels 4 and 5 (Suárez River basin).

4.2.2 k_{sn} map

The k_{sn} map (Fig. 8) displays along-channel variation in the steepness index within the Sogamoso and Lebrija drainage basins. The Suárez and the Chicamocha Rivers are characterized by low k_{sn} values (< 100 $m^{0.9}$) along their upper reaches, when they flow in the Chiquinquirà and Tunja highlands. They display high k_{sn} values (> 300 $m^{0.9}$) when they flow across the knickpoint at 2500 m and also for a long stretch before and after their confluence (Fig. 8). The western tributaries of the Suárez River commonly have high k_{sn} values at the confluence with the main river whereas the eastern tributaries display overall low k_{sn} values (< 200 $m^{0.9}$). The southernmost tributaries have high values (>200 $m^{0.9}$) where they cut across the main anticlines in the Mesas, but low values in the highlands (i.e. the Arcabuco anticline). The northernmost tributaries have generally medium to low k_{sn} values (~200 to < 200 $m^{0.9}$) with very low values (< 100 $m^{0.9}$) where they flow parallel to the main fold axes. In the Chicamocha drainage basin, downstream of the 2500 m knickpoint, the eastern tributaries commonly have medium to very high k_{sn} values (>200 $m^{0.9}$) and locally low (<100 $m^{0.9}$) k_{sn} values along their upper reaches. The western tributaries have k_{sn} between 100 and 200 all along their course, and locally high k_{sn} (> 200 $m^{0.9}$), highlighting the main knickzones.

High k_{sn} values (> 300 $m^{0.9}$) characterize the Lebrija River downstream of the confluence of the De Oro and Suratà Rivers when it incises through the Palonegro escarpment (Fig. 8). In the Lebrija River catchment, tributaries are relatively steep (k_{sn}>100 $m^{0.9}$) upstream of the Bucaramanga fault.

4.2.3 Drainage divide stability

The drainage divide stability results indicate a north-south gradient with a general instability to the north and stability to the south. In more detail, along the divide between the Lebrija and Sogamoso Rivers the segment 1 (DIV1 in Fig. 9) shows migration to the north, whereas segment 2 (DIV2 in Fig. 9) is almost stable. Along the divide between the Suárez and Chicamocha Rivers, the northern segments (DIV3, DIV4, DIV5 in Fig. 9) are slightly unstable, with a tendency to migrate towards the west (i.e. towards the Suárez River). Conversely, the southern segments (from DIV6 to DIV9 in Fig. 9), located in the Floresta Massif and the highlands, indicate clear stability.

4.2.4 Knickpoint celerity model

We modeled the propagation of two knickpoints located at ~1000 and ~1500 m of elevation along the longitudinal profiles of Suárez and Chicamocha Rivers with the starting point at 289 m of elevation (vertical projection of La Gacha windgap onto the Sogamoso River). The PDFs obtained for the knickpoint at 1500 m modeled in both the Suárez and Chicamocha Rivers suggest starting ages of 258±78 and 270 ±78 ka, thus with a strong agreement between the two rivers (Fig. 10). Conversely, the resulting PDFs for the knickpoint at 1000 m gave starting ages of 186±99 ka for the Suárez River and 216 ±100 ka for the Chicamocha River (Fig. 10).

To constrain the time of capture of the Suárez River by the Sogamoso River, we reconstructed the shape of the ancient river profiles starting from segments of the Suárez and Chicamocha Rivers (Fig. 11). In both rivers, the profile segment upstream of the knickpoint at 2500 m is geometrically incompatible with the windgap. Conversely, the modeling of the segments of the Suárez River upstream of the knickpoint at ~1500 and 1000 m provides ancient long profiles that approach the windgap elevation. Relying on the R^2 value, the knickpoint at 1500 m would be the best result. Nevertheless, the 1000 m-high knickpoint is geometrically better connected with the windgap, and the very low R^2 value is the result of a profile shape that deviates far from equilibrium. Using 186±99 ka as the capture age and the elevation difference between the windgap (850 m) and the present Sogamoso River channel just below the windgap (289 m), yields an incision rate of ~3 mm/yr.

5. Discussion

The overall topography and drainage pattern of the study area speak to a landscape in a transient state. The main trigger of this transience is likely the combination of regional uplift since the late Miocene (Hooghiemstra et al., 2006; Mora et al., 2008, 2015; Anderson et al., 2015) and of base-level fall in response to the reopening of the Magdalena Valley Basin to the north during the Pliocene (Silva et al., 2013; Struth et al., 2020). However, our observations indicate that the

dynamics of the rearrangement of the river network may not be entirely explained by the model proposed so far. Here, we propose a new model based on our observations with a bearing on the relative temporal sequence of river captures.

We consider short-term (< 10^6 yr) climate changes as likely negligible in the long-term landscape evolution. In fact, the oscillation between dry/cold and humid/warm conditions controls fluvial aggradation and incision whose time scale (10^5 yr) is shorter than both the response time of river systems (10^5-10^6 yr) and tectonic forcing (10^6 yr) (Whipple, 2001).

5.1 The regional drainage divide

At a regional scale, in the Cocuy Sierra, the regional drainage divide between the westward and eastward flowing rivers is shifting westwards towards the highest peaks (Fig. 5a). To the south, it is almost coincident (Fig. 5b), and further south shifting to the east (Fig. 5c). Given the high amount of mean annual precipitation (Hijmans et al., 2005; Fig. S1 supplementary material) and higher erosion rates measured on the eastern side of the EC (Struth et al., 2017), the position of the regional divide compared to the topography indicates that the Orinoco River tributaries are more intensely incising the topography than those of the Chicamocha River, as confirmed by the very high values of slope and local relief on the eastern flank of Cocuy Sierra (Figs. 2; 5; 6). The eastward shift in the southern portion could be possibly related to local orographic/precipitation variations as there the eastern Orinoco River tributaries are strongly incising the EC slope (Mora et al., 2008). Conversely, on the western flank, although the values of slopes and local relief (Figs. 2; 5; 6) are high, the regional drainage divide between the Suárez and Magdalena rivers generally coincides with the maximum elevation displaying small and not significant shifts (Fig. 5).

In the interior of the EC, the high values of local relief (Fig. 6) do not coincide with the highest topography, indicating that fluvial incision has not yet reached the highest elevations (Santander Massif and Cocuy Sierra) and the highlands (Chiquinquirà and Tunja). In fact, along the northern swath profile, the local relief is high everywhere (Fig. 5a), suggesting that all of the northern sector rivers are equally responding to the same forcing. In the central sector, values of slope and local relief (Figs. 2; 5; 6) are locally high but the regional drainage divide between the Suárez and Magdalena Rivers generally coincides with the maximum elevation displaying small and not significant shifts (Fig. 5). The highlands in the south, at elevations above 2500 m, are characterized by very low values of local relief (Fig. 5b, c) indicating that they have not been affected by river incision. Here, the longitudinal profiles of some rivers (channels 1, 2, 6, 7, 8; Fig. 7) show an upper concave segment that records a previous equilibrium state with a base level different from the present one. Erosion rates evaluated from the concentration of cosmogenic ^{10}Be in modern fluvial

deposits in both the Chiquinquirà and Bogotá highland are lower than 0.02 mm/a (Struth et al., 2017), thereby indicating that this area has not yet adjusted to the new base level.

5.2 The low-relief highlands (Upper Paleolandscape)

The Chiquinquirà and Tunja highlands, as well as the southern Bogotá one, are low relief areas that in the past were internally drained as recorded by the extensive presence of Plio-Pleistocene lake deposits (Torres et al., 2005; Sarmiento et al., 2008; Vriend et al., 2012). In the Chiquinquirà highland the maximum outcropping area of the lake deposits (Vriend et al., 2012) indicates that in the recent past the lake filled the valley. Most likely, the filling of the Chiquinquirà highland has been caused by damming of the Suárez River due to large landslides that are located along the river valley close to its exit from the highland (Fig. 3g), in contrast to a formerly proposed periglacial colluvium (Sarmiento et al. 2008). The Fúquene lake is likely the remnant of a larger lake that filled the Chiquinquirà highland which was subsequently progressively drained as the Suárez River incised a landslide dam (Vriend et al., 2012). In the Tunja highland, there is no record of lake deposits (Servicio Geológico Colombiano, 2015), but the landscape is similar to the adjacent Chiquinquirà highland. The valleys are wide, filled by fluvial deposits, and separated by small ridges. The knickpoints at 2500 m of elevation along the rivers that drain both the Chiquinquirà and Tunja highlands (channels 1 and 6 in Fig. 7) indicate the present position of an erosion wave related to a base-level fall. It is interesting to note in Fig. 7c that, although the highland edge knickpoint has the same elevation in both channels 1 and 6, the χ value for the Suárez River is much lower than that of the Chicamocha River, suggesting a gain of drainage area. Moreover, the downstream segment of the Suárez River is steeper, deviating from the trend of the other studied rivers. This configuration indicates the uplift of a plateau where part of the internal hydrography is captured by a river (Giachetta and Willett, 2018). The k_{sn} map shows high values of steepness downstream of the 2500 m knickpoint, which contrasts with the very low values on the highlands, thus underlining the influence of uplift and piracy on rivers (Fig. 8). On the footwall of the Boyacá fault, the western Chicamocha River tributaries flow in small perched alluvial valleys that possibly belong to the landscape of the highlands (Fig. 2b).

In the Chiquinquirà highland, the southern tip of the Arcabuco anticline is incised by two rivers that have a small drainage area upstream from the fold (Fig. 3h). We speculate that the modern drainage area of these rivers is too small to provide enough discharge to incise across the wide Arcabuco anticline. Instead, it is possible that they used to have a larger drainage area encompassing part of the Tunja highland. Thus, during the growth of the Arcabuco anticline, the rivers had an erosion rate equal to or higher than the uplift rate of the anticline and incised the two

antecedent valleys. This inference is supported by the observation that several other rivers incise the western flank of the Arcabuco anticline but none of them have breached the eastern limb of this fold. For example, channels 3 and 6 in Fig. 2 and of the rivers that incise the section of the Arcabuco anticline exposed in the Floresta Massif.

5.3 The Mesas (Lower Paleolandscape)

The landscape of the Mesas preserves the record of the competition between the Suárez and the Chicamocha Rivers comprising remnant landscapes, windgaps, and unstable divides.

Remnant landscapes

The rivers draining the western side of the Floresta Massif flow to the west, away from the highest peaks, in the hangingwall of the Boyacá fault. The longitudinal profile of one of these rivers, channel 4 (Figs. 2 and 7), is concave upstream from a knickpoint at ~1100 m, which marks its exit from the gently west-dipping Mesa de Barichara. This suggests that channel 4 was in equilibrium with the low-relief landscape of the Mesas, whose base level was lower in elevation than the highland's base level. Thus, the Floresta Massif was already a drainage divide when the low-relief landscape, which now forms the highlands, was wider than today. This is confirmed by the drainage divide stability analysis (Fig. 9) between the Suárez and the Chicamocha rivers. To the north, the tributaries of the Chicamocha River are more aggressive than those of the Suárez River, whereas to the south, the divide tends to be stable. In other words, the downstream tributaries are in disequilibrium in response to one or more erosion waves, possibly related to the Sogamoso River capture or previous events. Upstream, these erosion waves have not yet arrived.

The Mesa de Barichara, Mesa de Los Santos, and Mesa de Ruitoque are remnants of an older landscape whose almost flat morphology is strongly influenced by the sub-horizontal layering of the underlying rock. The Mesas, described as part of an erosional surface gently tilted to the north and the west (Julivert, 1958), are younger than the highland's paleolandscape. In the southernmost Mesa de Barichara, the underlying rocks are folded and the eastern tributaries of the Suárez River flow mainly along the syncline axis. Locally they cut across anticlines forming a knickpoint (channel 3 in Fig. 2; high values of k_{sn} in Fig. 8). To the north, the longitudinal profiles of the eastern tributaries of Suárez River display a knickpoint when they exit from the Mesa old landscape (Figs. 7 and 8).

Windgaps, unstable divides, and fluvial network organization

Along the divide between the Suárez and the Chicamocha Rivers, at the eastern edge of the Mesa de Barichara, two windgaps are preserved (Fig. 4a). Alluvial deposits (head of channel 5, Boquerón River; Fig. 2) indicate that one of these windgaps hosted a river that sourced further east. These sediments are composed of well-sorted coarse sands interbedded with subordinated and discontinuous levels of poorly-sorted, sub-angular, and sub-rounded pebbles (Fig. 4c-f). The depositional environment was likely a trunk channel filled by fluvial sands alternating with colluvial/debris-flow gravels. The detritus is composed of granitic and sedimentary rock fragments. The windgap is incised within the Cretaceous sedimentary sequence and it is part of a valley where no granitic rocks are exposed at present. Jurassic granodioritic rocks are exposed in the neighboring Chicamocha drainage basin to the east at a lower elevation than the Boquerón windgap and across the Chicamocha River (Figs. 1c). Thus, a river sourced partly in the granitic rocks to the east of the Boquerón windgap fed the hanging valley. The intense weathering of the deposit also provides further evidence of a remnant of an older landscape.

The Boquerón windgap is oriented in the same direction as the rivers flowing from the southern Santander Massif (channels 13 and 14 in Fig. 2). This suggests that the Boquerón River valley (channel 5) and its windgap were part of a river draining the southern Santander Massif and flowing to the west into the Suárez River. Although channel 13 (Fig. 2, Guaca River) is directly to the east of the windgap, it is not possible to infer an original connection between them since offset along the Bucaramanga fault should have displaced the original drainage. Moreover, the longitudinal profiles of the rivers draining the southern Santander Massif do not show an older reach that could suggest a previous connection, but the stronger incision of the Chicamocha River could have eroded any older features. The Chicamocha River and its tributaries have steep channels (Fig. 8) and rectilinear longitudinal profiles (Fig. 7) where thick alluvial sediments bury any older landscape features. Nevertheless, the Boquerón River windgap, as a remnant of an older drainage network, indicates that at the very least a river flowed from the southern Santander Massif to the west passing across and above the present location of the Chicamocha River. This inference is in line with the drainage divide observations where sections 4 and 5 of the divide between the Suárez and Chicamocha Rivers are unstable and migrating towards the Suárez drainage basin (Fig. 9). Referring to divide section 5 (Fig. 9), we exclude that the different rock susceptibility to erosion may have any control on the migration of the divide. Following the model by Zondervan et al. (2020), the divide on exhumed basement rock should migrate towards the center of highly resistant rocks. Conversely, divide section 5 migrates southwestward towards sedimentary erodible rocks (Figs. 1c and 9). Thus, the Chicamocha River acts as an aggressor at the expense of the Suárez River drainage basin, where

the downstream portion of the Chicamocha River valley is younger than that of the downstream area of the Suárez River.

The χ plots of the Chicamocha River and its western tributaries (Fig. 7c) do not show an increase in drainage area but rather they have similar χ values at the highland edge knickpoint. This suggests that channels 6 (Chicamocha River), 7, and 8 already drained the highlands before the Chicamocha River started to erode aggressively along its lower modern downstream reach. Collectively, our observations indicate that originally the Chicamocha River was not flowing to the north as suggested by Julivert (1958) and Struth et al. (2020) and that the upper portion of the Chicamocha River was possibly a Suárez River tributary (Fig. 12). In this scenario, the elbow of the Chicamocha River close to the Mesas de Los Santos would not be indicative of a northward flow. Instead, it likely results from the intersection of the older drainage network (flowing down from the Santander Massif) and the more recent Chicamocha path. Finally, the eastern tributaries of the Chicamocha River have high steepness, similar to the lower segment of the Chicamocha River, and in general, are steeper than the Suárez River tributaries. This behavior could be related to the higher and more recent uplift of the Cocuy Sierra relative to the adjacent western area as indicated by its higher topography and higher erosion rates since the late Miocene (Siravo et al., 2018, 2019).

In contrast to the Chicamocha River, the Suárez River did not change route significantly, except along its lowermost reach. Considering the several knickpoints downstream of the highlands, the Suárez River (channel 1) and probably channel 2 likely drained portions of the highlands before the events that caused the drainage reorganizations. The lower χ value of the Suárez River knickpoint at 2500 m is related to the integration of larger portions of the highlands into its drainage basin (Fig. 7c). The other knickpoints of the Suárez River at ~1000 m and ~1500 m (Figs. 2c and 7) indicate two additional erosional waves. Constraints on these events come from the paleo-profile modeling where the paleo-profile of the Suárez River upstream of the 1500 m knickpoint is ~200 m higher than the present La Gacha River, which is instead geometrically connected to the paleo-profile upstream of the ~1000 m knickpoint (Fig. 11). Thus, we suggest that as the Suárez River integrated a large portion of the highlands into its drainage, flowing on the Mesas to the north into the present Lebrija River basin. This is based upon: 1) the instability of the divide between the Sogamoso and the Lebrija Rivers and its northward migration (Fig. 9); 2) the 5 km wide and 500 m deep windgap located along their divide (Fig. 3c); and 3) the extensive fluvial deposits outcropping north of the windgap (Fig. 3e), as well as the width of the downstream valley (Fig. 3d). These features cannot be related to the ephemeral La Gacha River but to a river with a much higher discharge. This drainage configuration was disrupted by two subsequent river capture events. In contrast to the model by Struth et al. (2020), we interpret these captures as causing two erosional waves. The first erosional

wave (marked by the knickpoint at 1500 m), could be related to the opening of the Bucaramanga depression after the capture of the Lebrija River at 260-270 ka (Fig. S7 and 10). This event could have also enhanced the subsequent incision of the Los Cobardes anticline by the Lebrija River, which is documented by the gorge and the channel steepness downstream the knickpoint at 600 m (Figs. 7b, d). The second erosional wave, marked by the knickpoint at 1000 m (Fig. 7), is related to the Sogamoso piracy that likely occurred between 186 and 216 ka (Fig. 10). The strong incision resulting from this piracy is recorded in the Suárez River long profile where a rectilinear segment is present downstream of the knickpoint at 1000 m. Additionally, very high values of steepness index also characterize the lower reach of the Chicamocha River (Figs. 7, 8). The fact that the Sogamoso River took more time to incise the Los Cobardes anticline could be related to a differential topographic expression as the Lebrija River cuts the northern tip of the fold where the topography is less marked.

Julivert (1958) proposed that the area between the Bucaramanga and Suárez faults was a subsiding block where eroded material from the Santander Massif, the Palonegro escarpment, and the southern Mesas accumulated to form the present Bucaramanga alluvial fan. In this interpretation, both the Suárez and Chicamocha Rivers were flowing north into the present Lebrija drainage basin, and after depositing the Bucaramanga alluvial fan, they continued to the north following the Bucaramanga fault. Some hanging benches at ~1200 m elevation south of Cepità (approximatively south of the confluence of channel 14; Fig. 2a) along the Chicamocha River valley are proposed as remnants of an older Chicamocha River course (Julivert, 1958). However, no sedimentologic nor morphologic description for these benches is reported and their field location and confirmation is uncertain. The Sogamoso-Lebrija divide east of the Mesa de Los Santos is stable, suggesting that no significant drainage area changes occurred (Fig. 9). North of the city of Bucaramanga and to the east of the Mesa de Los Santos, there is no fluvial valley along the Bucaramanga fault (Fig. 3c). Finally, no abandoned deposits are preserved to the east of the Mesa de Los Santos and Mesa de Ruitoque.

In our model, the Suárez River, before being captured by the Sogamoso River, contributed to the formation of the Bucaramanga alluvial fan, which is older than the windgap deposit (Jimenez et al., 2015; Struth et al., 2020). The sedimentary succession of the alluvial fan, composed by a basal alluvial level, an alluvial to lacustrine middle layer, and an upper conglomeratic and sandy portion (Julivert, 1958; De Porta, 1959), indicates a transition from an alluvial plain and possibly a closed drainage basin with a lake to a high energy fluvial environment. Thus, it is possible that the old Suárez River and its tributaries, including the Chicamocha River, and other rivers flowing from the Santander Massif into the Bucaramanga depression deposited the lowermost part (Organos and

Finos members) of the Bucaramanga alluvial fan. A general fluvial environment could have sporadically developed into a closed drainage basin with the formation of a lake following the activity of the Suárez and Bucaramanga faults. The Suratà River could have deposited most of the conglomeratic and sandy upper portion of the fan (Gravoso and Limos Rojos members). Indeed, the morphology of the northernmost part of the alluvial fan indicates an eastern provenance. Paleo-current data could provide further clues to solve the Bucaramanga alluvial fan genesis. Unfortunately, the available provenance data provide contrasting interpretations between an eastern or southern source position (Plata-Guerrero and Moreno-Ruiz, 2015; Solano 2016).

5.4 Landscape evolution, plateau integration and fluvial reorganization in the Eastern Cordillera

Based on the described data, we propose a conceptual model of the landscape evolution of the study area (Fig. 12). The deformation of the EC started in the Paleogene and has increased since the middle-late Miocene, progressively migrating to the east (Bayona et al., 2008; Parra et al., 2009; 2012; Caballero et al., 2013; Siravo et al., 2018; Bayona et al., 2020). During this time, a low relief landscape developed in the EC (e.g. Hooghiemstra et al., 2006; Silva et al., 2013). The rivers shaped wide valleys in between small ridges formed by the growing anticlines. The early exhumed Los Cobardes anticline (Parra et al., 2012) controlled the Suárez River pattern as it flowed northward, parallel to the topographic barrier and collecting waters from the eastern tributaries (Fig. 12a). The Suárez River was possibly able to cross the topographic barrier of the Los Cobardes Anticline at its northern tip where elevation is lower to join downstream with the Magdalena River. Although uplift and exhumation characterized the Santander Massif and Cocuy Sierra in the Oligocene (Mora et al. 2015; Siravo et al, 2018), since the late Miocene, an increase in uplift (Hooghiemstra et al., 2006; Anderson et al., 2015) and exhumation (Mora et al., 2015, 2008; Siravo et al., 2018) combined with a base-level drop within the Magdalena River basin after the Early Pliocene (Silva et al., 2013) induced several erosion waves that deeply modified the landscape (Struth et al., 2020). During the Late Pliocene, the Chicamocha River and some rivers sourcing in the southern Santander Massif were tributaries of the Suárez River, including the one that shaped the present windgap of the Boquerón River (Fig. 12a). The Suárez River flowed northward into the Bucaramanga depression which at that time was filling with fluvial and lacustrine deposits (Fig. 12a-b). At the same time, the highlands were partly configured as closed intermontane basins filling with lacustrine and fluvial sediments. The first erosional wave that affected this landscape is marked by the knickpoints at ~ 2500 m along the Suárez and Chicamocha rivers. This could have caused the opening of the intermontane basin in the highlands. This phase could also correspond to

the time when the Mesas' landscape was shaped (Fig. 12a-b). Significant changes in the river routes occurred during the late Pleistocene after the deposition of the La Gacha windgap fluvial deposits at 409 ka. Deposition occurred in response to two erosional waves at ~260-270 ka, marked by the knickpoint at ~1500 m, and at 190-220 ka marked by the knickpoint at ~1000 m. The first erosional wave may be related to the opening of the Bucaramanga depression by headward erosion along the Lebrija River and the second to the capture of the Suárez River by the Sogamoso River that cut off the connection between the Bucaramanga depression and the Chicamocha-Suárez drainage (Fig. 12c).

6. Conclusions

High-standing plateau are common features in several mountain chains. In the central Andes, the Puna-Altiplano is internally drained and characterized by high aridity that at least partially enhanced its preservation. In the northern Andes, we investigated the complex drainage network and landscape evolution of the northern Eastern Cordillera of Colombia, where a high-standing plateau is presently exorheic. Here, different forcing factors are likely to have controlled the dynamic landscape reorganization. Two relict landscapes are preserved at elevations of ~2500 m (Chiquinquirà, Tunja and Bogotá highlands) and ~1500 m (Mesas) in the axial portion of the Eastern Cordillera, as evidenced by rivers longitudinal profiles, χ plots, and knickpoints analysis of the main rivers in the Sogamoso drainage basin. Additionally, abandoned fluvial deposits, windgaps, strongly incised valleys, and river elbows indicate transient state and ongoing landscape reorganization.

Previous reconstructions propose a post-Early Pliocene base-level fall (Struth et al., 2020) and exclude the Mesas landscape from the reconstruction. Conversely, we show that this relic landscape occupies a large portion of the mountain belt and preserves crucial features of the EC landscape evolution.

Our new evolutionary model implies that:

1) during the middle/late Pliocene, the Chiquinquirà highland was a closed drainage, while the Tunja highland was already drained by the Chicamocha River The routing of the Suárez River was controlled by the early exhumed Los Cobardes anticline. The river flowed northward into the Bucaramanga depression, parallel to the topographic barrier and collecting waters from the eastern tributaries, also draining the southern Santander Massif. The Chicamocha River was a Suárez tributary and its present lowermost portion was not developed yet. The Bucaramanga depression filled with fluvial and lacustrine deposits (lower Bucaramanga Fm.).

2) increased surface uplift in the Pliocene induced: 1) the Chiquinquirà highland opening in the early Pleistocene, which was captured by the Suárez River; and 2) the Mesas landscape development.

3) in the Late Pleistocene the Lebrija River captured the Suárez River at ~260-270 ka. The Sogamoso capture of the Suárez River at ~190-220 ka, truncated the connection between the Bucaramanga depression and the Suárez drainage, and finally led to the incision of the Mesas landscape and the formation of the present path of the Chicamocha River.

Finally, we reconstructed the complex history of a landscape in an active mountain belt. The EC case suggests that crustal architecture resulted from tectonic deformation strongly influenced the drainage pattern. Afterward, sub-crustal related surface uplift drives base-level lowering resulting in river captures, plateaux integration into the fluvial network, and an overall drainage re-organization.

Acknowledgments

We are grateful to Giovanny Jimenez and German Bayona for field support. We thank the editor Martin Stokes, Sarah J. Boulton, and two anonymous reviewers the helpful revisions. This research was funded through the MIUR Ph.D. fellowship awarded to GS.

References

Amaya, S., Zuluaga, C. A., & Bernet, M. (2017). New fission-track age constraints on the exhumation of the central Santander Massif: Implications for the tectonic evolution of the Northern Andes, Colombia. Lithos, 282, 388-402.

Anderson, V. J., Saylor, J. E., Shanahan, T. M., & Horton, B. K. (2015). Paleoelevation records from lipid biomarkers: Application to the tropical Andes. Bulletin, *127*(11-12), 1604-1616.

Ayala-Calvo, C., Bayona, G., Cardona, A., Ojeda, C., Montenegro, O., Montes, C., Valencia, V., Jaramillo, C., 2012. The Paleogene synorogenic succession in the northwestern Maracaibo block: tracking intraplate uplifts and changes in sediment-delivery systems. J. S. Am. Earth Sci. Special Ed. Tect. Clim. Shap. North. Andes South. Caribb. margin 39, 93e111. http://dx.doi.org/10.1016/ j.jsames.2012.04.005.

Bayona, G., Baquero, M., Ramírez, C., Tabares, M., Salazar, A. M., Nova, G., ... & Rodríguez, G. (2020). Unravelling the widening of the earliest Andean northern orogen: Maastrichtian to early Eocene intra-basinal deformation in the northern Eastern Cordillera of Colombia. Basin Research. https://doi.org/10.1111/bre.12496

Bayona, G., Cardona, A., Jaramillo, C., Mora, A., Montes, C., Caballero, V., & Mesa, A. (2013). Onset of fault reactivation in the Eastern Cordillera of Colombia and proximal Llanos Basin; response to Caribbean–South American convergence in early Palaeogene time. Geological Society, London, Special Publications, 377(1), 285-314.

Bayona, G., Cortés, M., Jaramillo, C., Ojeda, G., Aristizabal, J. J., & Reyes-Harker, A. (2008). An integrated analysis of an orogen–sedimentary basin pair: Latest Cretaceous–Cenozoic evolution of the linked Eastern Cordillera orogen and the Llanos foreland basin of Colombia. Geological Society of America Bulletin, 120(9-10), 1171-1197.

Beaumont, C., Muñoz, J. A., Hamilton, J., &Fullsack, P. (2000). Factors controlling the Alpine evolution of the central Pyrenees inferred from a comparison of observations and geodynamical models. Journal of Geophysical Research: Solid Earth, 105(B4), 8121-8145.

Berlin, M. M., & Anderson, R. S. (2007). Modeling of knickpoint retreat on the Roan Plateau, western Colorado. Journal of Geophysical Research: Earth Surface, 112(F3).

Boinet, T., Bourgois, J., Mendoza, H., & Vargas, R. (1989). La Falla de Bucaramanga (Colombia), su función durante la Orogenia Andina. Geol. Norandina, 11, 3-10.

Bueno, E., Solarte, A. (1994) Geología, Geotecnia y Comportamiento Erosivo del Área de Reserva Forestal de Bucaramanga. Tesis para optar al título de Geólogo. Escuela de Geología, UIS, Bucaramanga (1994)

Caballero, V., Mora, A., Quintero, I., Blanco, V., Parra, M., Rojas, L. E., Lopez C., Sanchez N., Horton B.K., Stockly D. & Duddy, I. (2013). Tectonic controls on sedimentation in an intermontane hinterland basin adjacent to inversion structures: The Nuevo Mundo syncline, Middle Magdalena Valley, Colombia. Geological Society, London, Special Publications, 377(1), 315-342.

Campbell, C.J., 1965. The Santa Marta wrench fault of Colombia and its regional Setting. In: Fourth Caribbean Geological Conference. Memoir, pp. 247-261 (Trinidad).

Cediel, F., R. P. Shaw, and C. Cáceres, (2003), Tectonic assembly of the Northern Andean Block, in C. Bartolini, R. T. Buffler, and J. Blickwede, eds., The Circum-Gulf of Mexico and the Caribbean: Hydrocarbon habitats, basin formation, and plate tectonics: AAPG Memoir 79, p. 815–848.

Cooper, M. A., Addison, F. T., Alvarez, R., Coral, M., Graham, R., Hayward, B. A., Howe, S., Martinez, J., Naar, J., Penas, R., Pulham, A. J., Taborda, A. (1995). Basin development and tectonic history of the Llanos Basin, Eastern Cordillera, and middle Magdalena Valley, Colombia. AAPG bulletin, 79(10), 1421-1442.

Crosby, B. T., & Whipple, K. X. (2006). Knickpoint initiation and distribution within fluvial networks: 236 waterfalls in the Waipaoa River, North Island, New Zealand. Geomorphology, 82(1-2), 16-38.

De Porta, J., 1959. La Terraza de Bucaramanga. UIS. Bol. de Geología No. 3, pp. 5e13 (Bucaramanga).

Diederix, H., Hernandez, C., Eliana, M.T., Osorio, J.A., Botero, P., 2009. Memorias Congreso Colombiano de Geologia, Paipa- Boyaca. Resultados preliminares del primer estudio paleosismológico a lo largo de la falla de Bucaramanga.

Dörr, W., Grösser, J. R., Rodriguez, G. I., & Kramm, U. (1995). Zircon U-Pb age of the Paramo Rico tonalite-granodiorite, Santander Massif (Cordillera Oriental, Colombia) and its geotectonic significance. Journal of South American Earth Sciences, 8(2), 187-194.

Fabre A.D. (1981). Geología regional de la Sierra Nevada del Cocuy, Plancha 137, "El Cocuy". Departamento de Boyaca e Intendencia de Arauaca. Informe No 1877, Ingeominas, Bogotà D.E. 1981.

Fabre, A., Osorio, M., Vargas, R., Etayo, F. (1985). Mapa geológico de la plancha 137 Cocuy Escala 1:100 000. ServicioGeológicoColombiano. Bogotá.

Flint, J. J. (1974). Stream gradient as a function of order, magnitude, and discharge. Water Resources Research, 10(5), 969-973.

Forte, A. M., & Whipple, K. X. (2018). Criteria and tools for determining drainage divide stability. Earth and Planetary Science Letters, 493, 102-117.

Gallen, S. F., Wegmann, K. W., &Bohnenstiehl, D. R. (2013). Miocene rejuvenation of topographic relief in the southern Appalachians. GSA Today, 23(2), 4-10.

García, Y.C., Añez, M., Struth, L., Tesón, E., Caballero, V. (2015). Rios Chicamocha y Suárez: un ejemplo de la evolución de la red de drenaje en orogénos de inversión. XV Congreso colombiano de geología, 2015 "Innovar en Sinergia con el Medio Ambiente" Bucaramanga, Colombia Agosto 31 – Septiembre 5, 2015.

Giachetta, E., & Willett, S. D. (2018). Effects of river capture and sediment flux on the evolution of plateaus: insights from numerical modeling and river profile analysis in the upper Blue Nile catchment. Journal of Geophysical Research: Earth Surface, 123(6), 1187-1217.

Giachetta, E., Molin, P., Scotti, V. N., & Faccenna, C. (2015). Plio-Quaternary uplift of the Iberian Chain (central–eastern Spain) from landscape evolution experiments and river profile modeling. Geomorphology, 246, 48-67.

Gilbert, G.K. (1877). Geology of the Henry Mountains. USGS Report, Government Printing Office, Washington, D.C.

Hack, J. T. (1973). Stream-profile analysis and stream-gradient index. Journal of Research of the US Geological Survey, 1(4), 421-429.

Hermelin, M. (2016). Geomorphological Landscapes and Landforms of Colombia. In Landscapes and Landforms of Colombia (pp. 1-21). Springer, Cham. https://doi.org/10.1007/978-3-319-11800-0_1

Hijmans, R.J., S.E. Cameron, J.L. Parra, P.G. Jones and A. Jarvis, 2005. Very high resolution interpolated climate surfaces for global land areas. International Journal of Climatology 25: 1965 - 1978.

Hooghiemstra, H., V. M. Wijninga, and A. M. Cleef (2006), The paleobotanical record of Colombia: Implications for biogeography and biodiversity,Ann.Supply and removal of sediment in a landslide-dominated mountain belt: Central Range, Taiwan. Journal of Geology, 108, 73–89.

Hovius, N., Stark, C. P., Hao-Tsu, C., & Jiun-Chuan, L. (2000). Supply and removal of sediment in a landslide-dominated mountain belt: Central Range, Taiwan. The Journal of Geology, 108(1), 73-89.

Howard, A. D. (1994). A detachment-limited model of drainage basin evolution. Water resources research, 30(7), 2261-2285.

Howard, A. D., & Kerby, G. (1983). Channel changes in badlands. Geological Society of America Bulletin, 94(6), 739-752.

Hubach, E. (1952). Interpretacion geologica de la erosion y de los deslizamientos en Bucaramanga, y medidas de defensa.Serv. Geol. Nal. Bogotá. Inf., 867 (1952), pp. 2-4.

IDEAM, Instituto de Hidrología, Meteorología y Estudios Ambientales (2001). Los glaciares colombianos, expresión del cambio climático global. Bogotá, D.C., IDEAM, 2001

Ingeominas, 2001. Zonificación Sismo Geotecnica Indicativa del Area Metropolitana De Bucaramanga, Fase II. Convenio realizado entre la CDMB e Ingeominas, Bucaramanga.

Ingeominas, 2008. Modelo de evolución morfotectonica cuaternaria basado en Evidencias estructurales, neotectónicas y paleosismológicas de los principales Sistemas de falla en la región de Bucaramanga. Diederix. H, Torres. E. M, Hernandez. C and Botero. P. A. Bogotà.

Irving, E.M., 1971. La evolución estructural de los Andes más septentrionales de Colombia. BoletínGeológico, Ingeominas, Bogotá 19 (2), 1e90.

Jiménez, G., Speranza, F., Faccenna, C., Bayona, G., & Mora, A. (2015). Magnetic stratigraphy of the Bucaramanga alluvial fan: Evidence for a ≤ 3 mm/yr slip rate for the Bucaramanga-Santa Marta Fault, Colombia. Journal of South American Earth Sciences, 57, 12-22.

Jiménez, G., Speranza, F., Faccenna, C., Bayona, G., & Mora, A. (2014). Paleomagnetism and magnetic fabric of the Eastern Cordillera of Colombia: Evidence for oblique convergence and nonrotational reactivation of a Mesozoic intracontinental rift. Tectonics, 33(11), 2233-2260.

Julivert, M. (1958). Geología de la zona tabular entre San Gil y Chiquinquirá Cordillera Oriental, Colombia. Boletín de Geología, 2.

Julivert, M. (1963). Nuevas observaciones sobre la estratigrafía y tectónica del Cuaternario de los alrededores de Bucaramanga. Boletín de Geología, (15), 41-59.

Kammer, A., Sánchez, J., 2006. Early Jurassic rift structures associated with the Soápaga and Boyacá faults of the Eastern Cordillera, Colombia: sedimentological inferences and regional implications. Journal of South American Earth Sciences 21, 412e422.

Kirby, E., & Whipple, K. (2001). Quantifying differential rock-uplift rates via stream profile analysis. Geology, 29(5), 415-418.

Kirby, E., & Whipple, K. X. (2012). Expression of active tectonics in erosional landscapes. Journal of Structural Geology, 44, 54-75.

Loget, N., & Van Den Driessche, J. (2009). Wave train model for knickpoint migration. Geomorphology, 106(3-4), 376-382.

Mackin, J. H. (1948). Concept of the graded river. Geological Society of America Bulletin, 59(5), 463-512.

Masek, J. G., Isacks, B. L., Gubbels, T. L., & Fielding, E. J. (1994). Erosion and tectonics at the margins of continental plateaus. Journal of Geophysical Research: Solid Earth, 99(B7), 13941-13956.

Molin, P., Pazzaglia, F. J., &Dramis, F. (2004). Geomorphic expression of active tectonics in a rapidly-deforming forearc, Sila massif, Calabria, southern Italy. American journal of science, 304(7), 559-589.

Mora, A., García, A., (2006). Cenozoic Tectono-stratigraphic relationships between the Cesar Sub-Basin and the Southeastern Lower Magdalena Valley Basin of Northern Colombia. In: AAPG 2006 Annual Convention. Houston, Texas.

Mora, A., Parra, M., Strecker, M. R., Sobel, E. R., Hooghiemstra, H., Torres, V., & Jaramillo, J. V. (2008). Climatic forcing of asymmetric orogenic evolution in the Eastern Cordillera of Colombia. Geological Society of America Bulletin, 120(7-8), 930-949.

Mora, A., Parra M., Forero G., Blanco V., Moreno N., and Caballero V., (2015). What drives orogenic asymmetry in the Northern Andes?: A case study from the apex of the Northern Andean Orocline, in C. Bartolini and P. Mann, eds., Petroleum geology and potential of the Colombian Caribbean Margin: AAPG Memoir 108, p. 547–586

París, G. M, Machette. R, Dart and K. Haller, (2000). Map and Database of Quaternary Faults and Folds in Colombia and its Offshore Regions. U.S. Department of the Interior U.S. Geological Survey. 66 p.

Parra, M., Mora, A., Sobel, E. R., Strecker, M. R., & González, R. (2009). Episodic orogenic front migration in the northern Andes: Constraints from low-temperature thermochronology in the Eastern Cordillera, Colombia. Tectonics, 28(4).

Parra, M., Mora, A., López, C., Rojas, L. E., & Horton, B. K. (2012). Detecting earliest shortening and deformation advance in thrust belt hinterlands: Example from the Colombian Andes. Geology, 40(2), 175-178.

Pazzaglia, F. J., & Brandon, M. T. (2001). A fluvial record of long-term steady-state uplift and erosion across the Cascadia forearc high, western Washington State. American Journal of Science, 301(4-5), 385-431.

Perron, J. T., &Royden, L. (2013). An integral approach to bedrock river profile analysis. Earth Surface Processes and Landforms, 38(6), 570-576.

Plata-Guerrero, C.,L., Moreno-Ruiz, S. N., (2015), Estudio sedimentológico del miembro organos en la formación bucaramanga, hacia el escarpe occidental en las estribaciones del municipio de Girón. Degree thesis. Universidad Industrial de Santander.

Reyes-Harker, A., Ruiz-Valdivieso, C. F., Mora, A., Ramírez-Arias, J. C., Rodriguez, G., De La Parra, F., Caballero, V., Parra, M., Moreno, N., Horton, B.K., Saylor, J.E., Silva, A., Valencia, V., Stockli, D., & Blanco., V. (2015). Cenozoic paleogeography of the Andean foreland and retroarc hinterland of Colombia. AAPG Bulletin, 99(8), 1407-1453

Sarmiento, G., Gaviria, S., Hooghiemstra, H., Berrio, J. C., & Van der Hammen, T. (2008). Landscape evolution and origin of Lake Fúquene (Colombia): tectonics, erosion and sedimentation processes during the Pleistocene. Geomorphology, 100(3), 563-575.

Sarmiento-Rojas, L. F., Van Wess, J. D., &Cloetingh, S. (2006). Mesozoic transtensional basin history of the Eastern Cordillera, Colombian Andes: Inferences from tectonic models. Journal of South American Earth Sciences, 21(4), 383-411.

Saylor, J. E., Horton, B. K., Stockli, D. F., Mora, A., &Corredor, J. (2012). Structural and thermochronological evidence for Paleogene basement-involved shortening in the axial Eastern Cordillera, Colombia. Journal of South American Earth Sciences, 39, 202-215.

Schwanghart, W., Kuhn, N. J. (2010): TopoToolbox: a set of Matlab functions for topographic analysis. Environmental Modelling & Software, 25, 770-781.

Servicio Geológico Colombiano (2015). Mapa Geológico de Colombia 2015. Escala 1:100.000; Compilado por Gómez Tapias, J., Montes Ramírez, N.E., Nivia Guevara, A. Y Diederix, H. Bogotá, 2015.

Sembroni, A., Molin, P., Soligo, M., Tuccimei, P., Anzalone, E., Billi, A., ... &Tarchini, L. (2020). The uplift of the Adriatic flank of the Apennines since the Middle Pleistocene: New insights from the Tronto River basin and the Acquasanta Terme Travertine (central Italy). Geomorphology, 352, 106990.

Sembroni, A., Molin, P., Pazzaglia, F. J., Faccenna, C., and Abebe, B. (2016). Evolution of continental-scale drainage in response to mantle dynamics and surface processes: An example from the Ethiopian Highlands. Geomorphology, 261, 12-29.

Silva, A., Mora, A., Caballero, V., Rodriguez, G., Ruiz, C., Moreno, N., ... & Quintero, I. (2013). Basin compartmentalization and drainage evolution during rift inversion: evidence from the Eastern Cordillera of Colombia. Geological Society, London, Special Publications, 377(1), 369-409.

Siravo, G., Fellin, M. G., Faccenna, C., &Maden, C. (2020). Transpression and the build-up of the Cordillera: the example of the Bucaramanga fault (Eastern Cordillera, Colombia). Journal of the Geological Society, 177(1), 14-30.

Siravo, G., Faccenna, C., Gérault, M., Becker, T. W., Fellin, M. G., Herman, F., & Molin, P. (2019). Slab flattening and the rise of the Eastern Cordillera, Colombia. Earth and Planetary Science Letters, 512, 100-110.

Siravo, G., Fellin, M. G., Faccenna, C., Bayona, G., Lucci, F., Molin, P., &Maden, C. (2018). Constraints on the Cenozoic deformation of the northern Eastern Cordillera, Colombia. Tectonics, 37(11), 4311-4337.

Solano L. 2016. Estudio de proveniencia de los sedimentos de la Formación Bucaramanga, al sur del río Frío; en los municipios de Floridablanca y Girón, Santander. Degree thesis. Universidad Industrial de Santander.

Stock, J. D., & Montgomery, D. R. (1999). Geologic constraints on bedrock river incision using the stream power law. Journal of Geophysical Research: Solid Earth, 104(B3), 4983-4993.

Struth, L. (2016). Evolution of fluvial drainage during mountain building in the eastern cordillera of Colombia (Doctoral dissertation, UniversitatAutònoma de Barcelona).

Struth, L., Teixell, A., Owen, L. A., &Babault, J. (2017). Plateau reduction by drainage divide migration in the Eastern Cordillera of Colombia defined by morphometry and 10Be terrestrial cosmogenic nuclides. Earth Surface Processes and Landforms, 42(8), 1155-1170.

Struth, L., Giachetta, E., Willett, S. D., Owen, L. A., & Tesón, E. (2020). Quaternary drainage network reorganization in the Colombian Eastern Cordillera plateau. Earth Surface Processes and Landforms, 45(8), 1789-1804.

Tesón, E., García, Y.C., Añez, M., Struth, L., Caballero, V., Babault, J. and Teixell, A. (2015). Capturas fluviales recientes de los ríos Chicamocha y Suárez: el origen de la terraza de Bucaramanga y causas de la reorganización de la red de drenaje. XV Congreso colombiano de geología, 2015 "Innovar en Sinergia con el Medio Ambiente" Bucaramanga, Colombia Agosto 31 – Septiembre 5, 2015.

Toro, J., 1990. The Termination of the Bucaramanga Fault in the Cordillera Oriental, Colombia. Masters thesis. University of Arizona, Department of Geosciences, Tucson.

Torres, V., Vandenberghe, J., & Hooghiemstra, H. (2005). An environmental reconstruction of the sediment infill of the Bogotá basin (Colombia) during the last 3 million years from abiotic and biotic proxies. Palaeogeography, Palaeoclimatology, Palaeoecology, 226(1), 127-148.

Tschanz, C., Marvin, R., Cruz, J., Mennert, H., Cebula, E., 1974. Geologic evolution of The Sierra Nevada De Santa Marta. Geol. Soc. Am. Bull. 85, 269e276.

van der Hammen, T. (1974). The Pleistocene changes of vegetation and climate in tropical South America. Journal of Biogeography, 3-26.

van der Hammen, T. (1985). The Plio-Pleistocene climatic record of the tropical Andes. Journal of the Geological Society, 142(3), 483-489.

van der Hammen, T., &Hooghiemstra, H. (2003). Interglacial–glacial Fuquene-3 pollen record from Colombia: an Eemian to Holocene climate record. Global and Planetary Change, 36(3), 181-199.

van der Lelij, R., Spikings, R., Ulianov, A., Chiaradia, M., & Mora, A. (2016). Paleozoic to Early Jurassic history of the northwestern corner of Gondwana, and implications for the evolution of the Iapetus, Rheic and Pacific Oceans. Gondwana Research, 31, 271-294.

Vargas, G., & Niño, A. (1992). Patrones de fracturamiento asociados a la Falla Bucaramanga. Universidad Industrial de Santander (Doctoral dissertation, Tesis, 95p).

Velandia, F. &Bermúdez, M.A. (2018). The transpressive southern termination of the Bucaramanga fault (Colombia): insights from geological mapping, stress tensors, and fractal analysis. Journal of Structural Geology, 115, 190–207, https://doi.org/10.1016/j.jsg.2018.07.020

Vriend, M., Groot, M. H. M., Hooghiemstra, H., Bogotá-Angel, R. G., &Berrio, J. C. (2012). Changing depositional environments in the Colombian Fúquene Basin at submillennialtime-scales during 284-27 ka from unmixed grain-size distributions and aquatic pollen. Netherlands Journal of Geosciences, 91(1-2), 199-214.

Whipple, K. X. (2001). Fluvial landscape response time: how plausible is steady-state denudation?. American Journal of Science, 301(4-5), 313-325.

Whipple, K. X. (2004). Bedrock rivers and the geomorphology of active orogens. Annu. Rev. Earth Planet. Sci., 32, 151-185.

Whipple, K. X., DiBiase, R. A., Ouimet, W. B., & Forte, A. M. (2017). Preservation or piracy: Diagnosing low-relief, high-elevation surface formation mechanisms. Geology, 45(1), 91-94.

Whipple, K. X., Hancock, G. S., & Anderson, R. S. (2000). River incision into bedrock: Mechanics and relative efficacy of plucking, abrasion, and cavitation. Geological Society of America Bulletin, 112(3), 490-503.

Whipple, K. X., & Tucker, G. E. (1999). Dynamics of the stream-power river incision model: Implications for height limits of mountain ranges, landscape response timescales, and research needs. Journal of Geophysical Research: Solid Earth, 104(B8), 17661-17674.

Whipple, K. X., & Tucker, G. E. (2002). Implications of sediment-flux-dependent river incision models for landscape evolution. Journal of Geophysical Research: Solid Earth, 107(B2), ETG-3.

Willett, S. D., McCoy, S. W., Perron, J. T., Goren, L., & Chen, C. Y. (2014). Dynamic reorganization of river basins. Science, 343(6175), 1248765.

Wobus, C., Whipple, K. X., Kirby, E., Snyder, N., Johnson, J., Spyropolou, K, Crosby, B., & Sheehan, D. (2006). Tectonics from topography: Procedures, promise, and pitfalls. Geological Society of America Special Papers, 398, 55-74.

Zondervan, J.R., Stokes, M., Boulton, S.J., Telfer, M.W. and Mather, A.E., 2020. Rock strength and structural controls on fluvial erodibility: Implications for drainage divide mobility in a collisional mountain belt. Earth and Planetary Science Letters, 538, p.116221.

FIGURE CAPTIONS

Figure 1: Tectonic setting of northern South America. a) Main plates and tectonics blocks interacting in the northern Andes. CP: Caribbean Plate; P-C: Panama-Choco Block; NP: Nazca Plate; SAP: South America Plate; WC: Western Cordillera; CC: Central Cordillera; MMV: Middle Magdalena Valley; EC: Eastern Cordillera; SM: Santander Massif; LB: Llanos Basin. b) Shaded topographic map of the Eastern Cordillera including main faults, rivers, and major drainage basins enclosed in black thick lines. Shaded rectangular areas show swath profile (Fig. 5) locations and extensions. c) Geologic map of the Eastern Cordillera (after Servicio Geológico Colombiano, 2015), main rivers (white lines; grey lines are drainage divides), and main identified knickpoints. 1: Quaternary; 2: Cenozoic; 3: Upper Cretaceous; 4: Lower Cretaceous; 5: Jurassic; 6: Jurassic igneous; 7: Paleozoic; 8: Proterozoic; 9: thrust or inverted faults; 10: strike slip faults; 11: faults; 12: anticline; 13: syncline. BAF: Bucaramanga Alluvial Fan; MR: Mesa de Ruitoque; MS: Mesa de los Santos; MB: Mesa de Barichara; CS: Cocuy Sierra; FM: Floresta Massif; TH: Tunja highland; CH: Chiquinquirà highland; BG: Bogotá highland; BU. F.: Bucaramanga Fault; SU. F.: Suárez Fault; BO. F.; Boyacá Fault; SO. F.: Soapaga Fault; LCA: Los Cobardes Anticline; Arc. A: Arcabuco Anticline.

Figure 2: Topographic expression of the EC and Santander Massif. a) Slope map and the analyzed rivers (blue lines). High values of slope are observed along the mountain range flanks and in the area incised by the Chicamocha River (channel 6) and the western flank of the Santander Massif. Low slope values are observed in the MMV and LB lowlands, and also in the central portion of the EC, at the highlands (CH and TH) and the Mesas (MB, MS, MR). b) Shaded topographic map. Main rivers together with main structures and drainage divide are shown. Shaded green and violet areas outline the relict upper (Highlands) and lower (Mesas) old landscapes. White boxes show the location of detailed observation from satellite images and field provided in figures 3 and 4. White lines are drainage divides.

Figure 3: Landforms of the Lebrija and Sogamoso River catchments. a.) Panoramic view of the Bucaramanga alluvial fan taken from the Palonegro escarpment. Notice the disconnection of the apex (BAF A.: Bucaramanga alluvial fan apex; vertical black arrow) from any possible feeding valley, the strong erosion of the distal part of the fan as well as the increase in elevation of the top surface to the east. The Bucaramanga and Suárez faults traces are outlined with vertical red arrows and bold red line, respectively. SM: Santander Massif; MR: Mesa de Ruitoque; MS: Mesa de Los Santos; PE; Palonegro escarpment. b) Field picture from the Mesa de Los Santos showing the horizontal layering of the Cretaceous succession and the intense erosion. c) The Bucaramanga alluvial fan (apex location indicated by concentric circles) and the Sogamoso-Lebrija drainage divide (red line). In the red circle, the windgap of the La Gacha River d) La Gacha River wind gap. e) 30 m-thick fluvial deposit found a few km to the north of the La Gacha River wind gap. Notice the alternation of gravel and sandy layers together with channel geometries. f) Panoramic view of the Lake Fúquene in the Chiquinquirà highland. h) Google Earth image (maps data: Google, Image Landsat/Copernicus; Image © 2021CNES/Airbus; Image © 2021 Maxar Technologies) (vertical exaggeration of factor 3) of the landslides found at the exits of the Suárez River from the Chiquinquirà highland, that possibly dammed the Suárez River. Black lines show the landslide crowns while white-shaded polygons are the bodies. The Suárez River is marked as a blue line. g) Two antecedent valleys cutting into the Arcabuco anticline. For symbolism and acronyms refer to Fig. 1.

Figure 4: Windgap at the Suárez /Chicamocha river divide. a) Northeastern edge of the Mesa de Barichara where two windgaps are observed. Only in the northern one (in the red circles) fluvial deposits are preserved b) Field picture of the Boquerón River (channel 5) windgap. c-f) The abandoned deposits show sedimentological features typical of alluvial facies interbedded with debris flow or mass transport.

Figure 5: Swath profiles across the EC (see location in Fig. 1b). The black line is the mean topography. The grey area marks the range between maximum and minimum elevation, and the arithmetical difference between them gives the local relief curve, in red. Main rivers and topographic features, as well as the location of the divides are pointed out. See text for detail. MMV: Middle Magdalena Valley; LCA: Los Cobardes anticline; MB: Mesa de Barichara; CS: Cocuy Sierra; Llanos Basin.

Figure 6: Local relief map of the northern EC and Santander Massif. High local relief values are found along main tectonic structures, whereas low values are found in the axial portion of the chain (Chiquinquirà (CH) and Tunja (TH) highlands and the Mesas (MB; MS; MR)), and outside of the chain (Middle Magdalena Valley (MMV) and Llanos Basin (LB) lowlands. For symbolism and acronyms refer to Fig. 1 and text.

Figure 7: Longitudinal profiles and χ plot of the Suárez and Chicamocha Rivers and tributaries (a; c) and of the Lebrija River and its tributaries (b; d). Chicamocha eastern tributaries (E) in pale magenta; western tributaries (W) in yellow. See the text for detailed description.

Figure 8: Map of the along-channel variation of the steepness index. Lower values characterize the highlands (CH and TH) and the Mesas (MB; MS; MR) tops whereas higher values are found at their boundaries. Additionally, high k_{sn} values are observed at the confluence of the Suárez and Chicamocha Rivers into the Sogamoso River, along main structural features and in the higher mountain ranges (CS, SM, FM). For acronyms refer to Fig. 1 and text.

Figure 9: Drainage divide stability analysis. The mute map indicates the analyzed sections of the divides between the Suárez, Chicamocha, and Lebrija drainage basins. The plot shows the variation across the divide of the four Gilbert parameters (Forte and Whipple, 2018) calculated along the selected divides sections (Figs. S2-S5 in the supplementary materials). The horizontal dashed line represents the stability condition of the divide. The direction of migration is predicted when a point falls above or below this line.

Figure 10: Probability Density Functions of the initiation times of the two knickpoints (~1000 and ~1500 m) modeled along the Suárez and Chicamocha Rivers as resulted from the knickpoint celerity model. See text for further explanation and Fig. S6 in the supplementary materials.

Figure 11: Paleo-longitudinal profiles of Suárez and Chicamocha Rivers reconstructed considering the segments upstream of the three main knickpoints (2500, 1500, and 1000 m) in the present longitudinal profiles. The projected paleo-longitudinal profile of the Suárez River relative to the knickpoint at 1000 m connects with the present Rio de Oro longitudinal profile and coincides with the wind gap (open star) at the divide between the Lebrija and Sogamoso drainage basins. The inset table reports the values of the main morphometric parameters of the three knickpoints and the R^2 resulted from the knickpoint celerity model. See text for further explanation.

Figure 12: Sketch model of the landscape evolution of the northern EC and Santander Massif. In panel D the background hillshade is for reference. LCA: Los Cobardes Anticline; SM: Santander Massif; FM: Floresta Massif; CS: Cocuy Sierra.

no competing interests to declare

Highlights

- Landscape evolution study of a high elevation intermontane plateau, northern Andes
- Applies topographic-hydrographic metrics to river systems and drainage divides
- Fluvial deposits, landforms and patterns suggest river-capture driven reorganization
- High elevation internally drained plateau configuration during Pliocene
- Plateau drainage captured by tectonically driven incision during Plio-Pleistocene

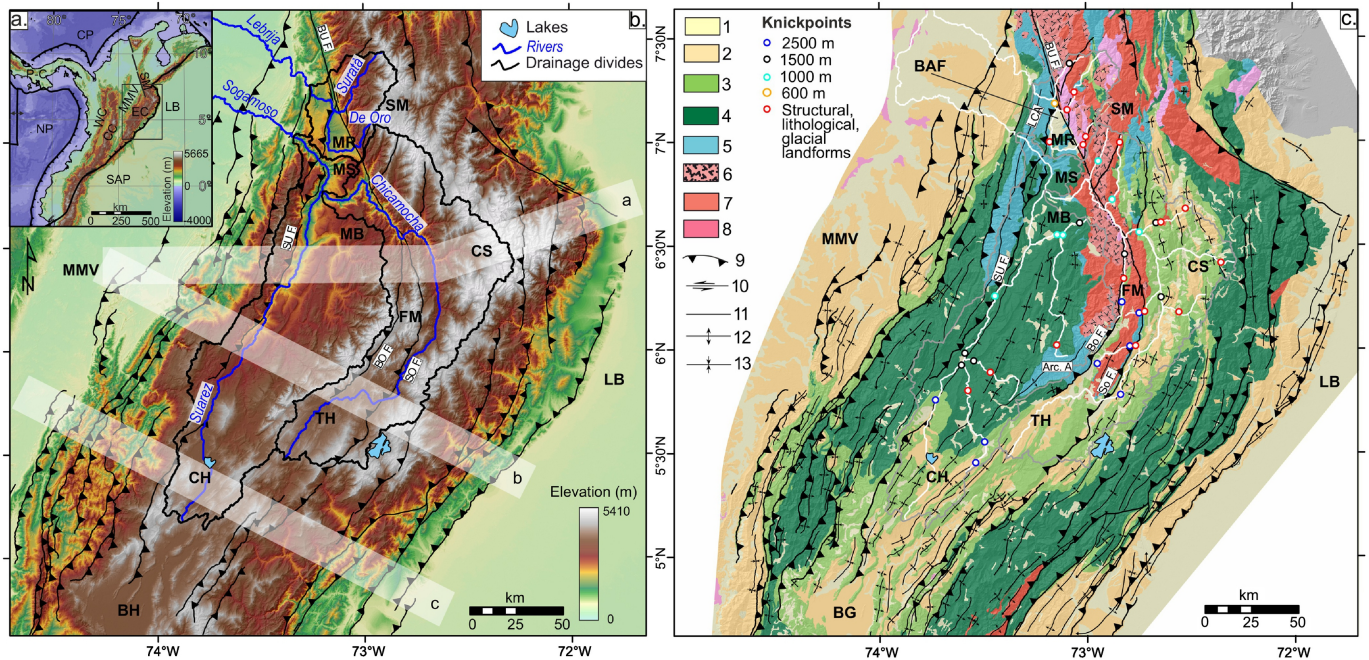
a.
b.
c.
Lakes
Rivers
Drainage divides
Lebrija
Sogamoso
Suarez
De Oro
Chicamocha
SUF
SM
MR
MS
MB
CS
FM
TH
CH
BH
MMV
LB
NP
CP
SAP
Elevation (m)
5665
0
-4000
5410
km
0 25 50
74°W
73°W
72°W
7°30N
7°N
6°30N
6°N
5°30N
5°N
Knickpoints
2500 m
1500 m
1000 m
600 m
Structural, lithological, glacial landforms
BAF
BG
Arc. A

Figure 1

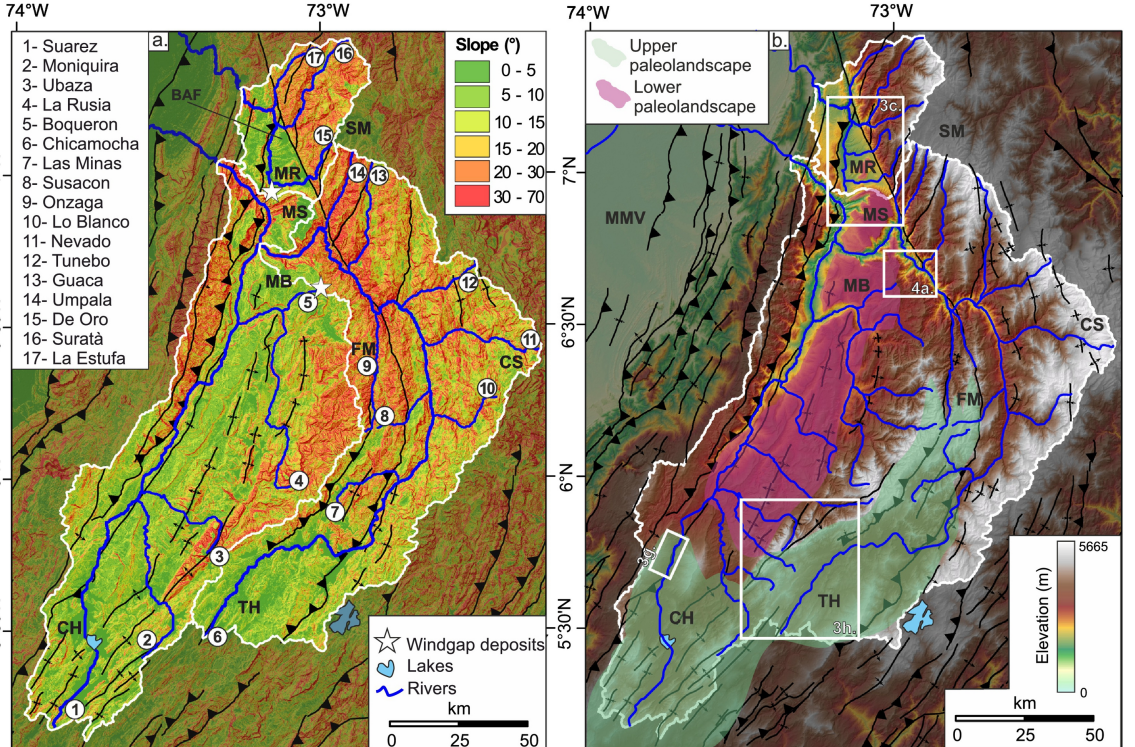
74°W
73°W
7°N
6°30'N
6°N
5°30'N
a.
b.
1- Suarez
2- Moniquira
3- Ubaza
4- La Rusia
5- Boqueron
6- Chicamocha
7- Las Minas
8- Susacon
9- Onzaga
10- Lo Blanco
11- Nevado
12- Tunebo
13- Guaca
14- Umpala
15- De Oro
16- Suratà
17- La Estufa
Slope (°)
0 - 5
5 - 10
10 - 15
15 - 20
20 - 30
30 - 70
Upper paleolandscape
Lower paleolandscape
BAF
SM
MR
MS
MB
FM
CS
MMV
CH
TH
3c.
4a.
3g.
3h.
Windgap deposits
Lakes
Rivers
km
0
25
50
Elevation (m)
5665
0

Figure 2

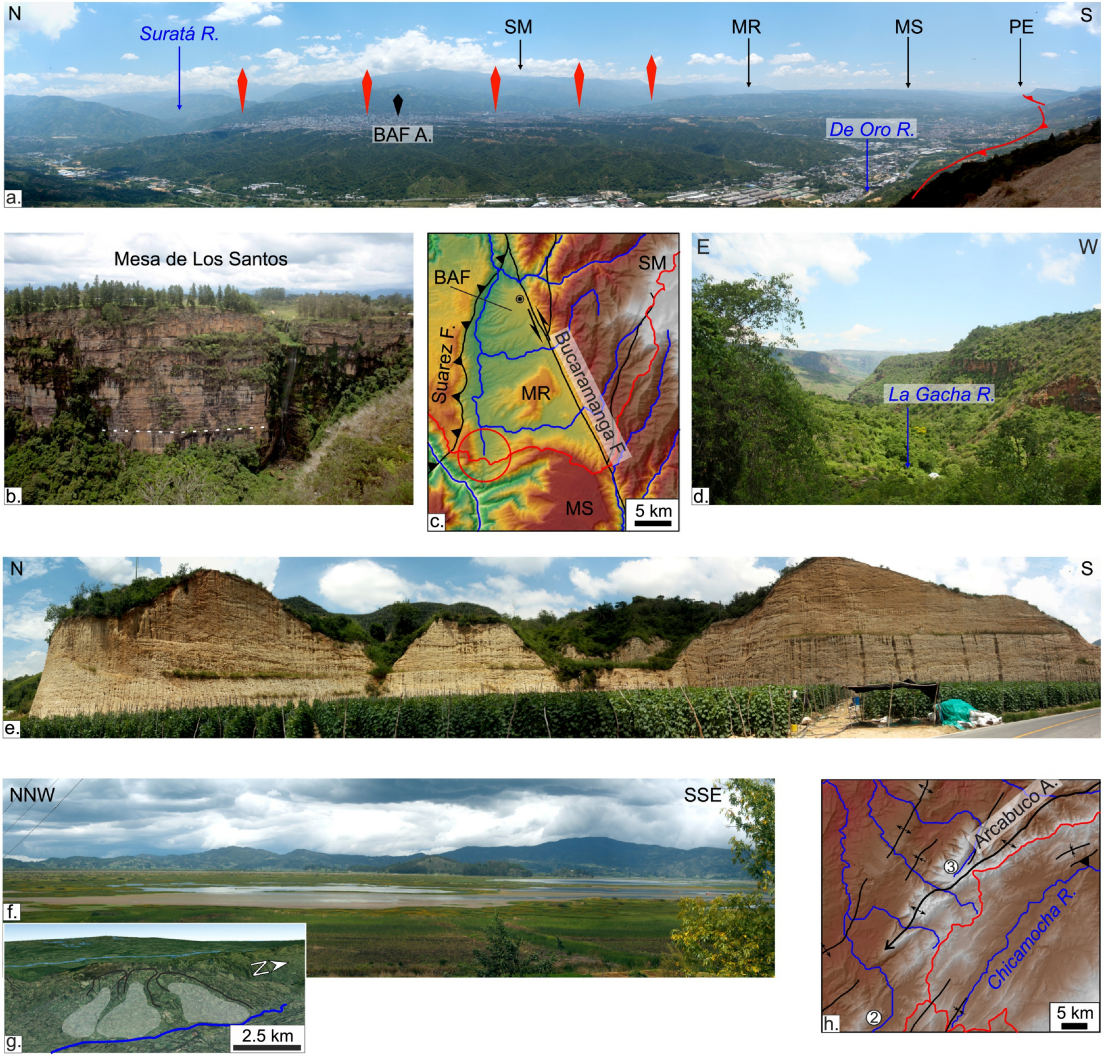
N
Suratá R.
SM
MR
MS
PE
S
BAF A.
De Oro R.
a.
Mesa de Los Santos
b.
BAF
SM
Suarez F.
Bucaramanga F.
MR
MS
5 km
c.
E
W
La Gacha R.
d.
N
S
e.
NNW
SSE
f.
Z
2.5 km
g.
Arcaburco A.
③
Chicamocha R.
5 km
h.
②

Figure 3

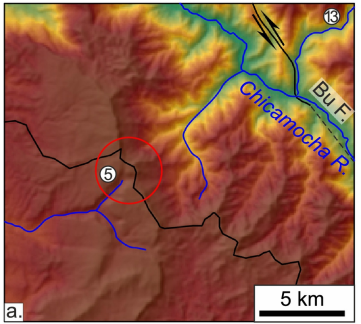

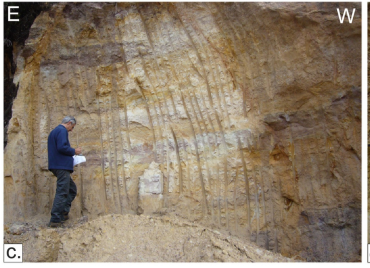

Figure 4

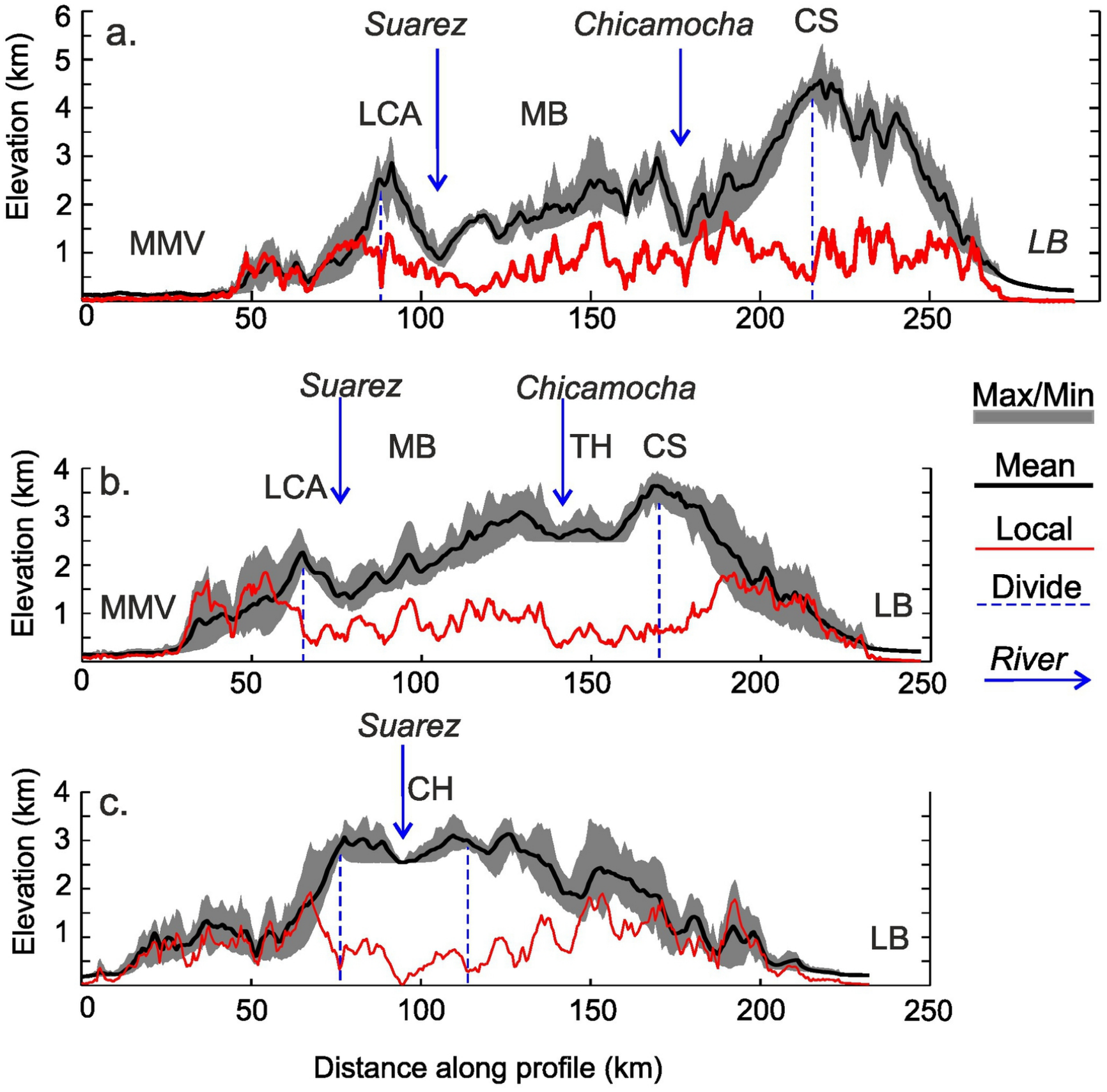
a.
Suarez
Chicamocha
CS
LCA
MB
MMV
LB
Elevation (km)
b.
Suarez
Chicamocha
MB
TH
CS
LCA
MMV
LB
Max/Min
Mean
Local
Divide
River
c.
Suarez
CH
LB
Distance along profile (km)

Figure 5

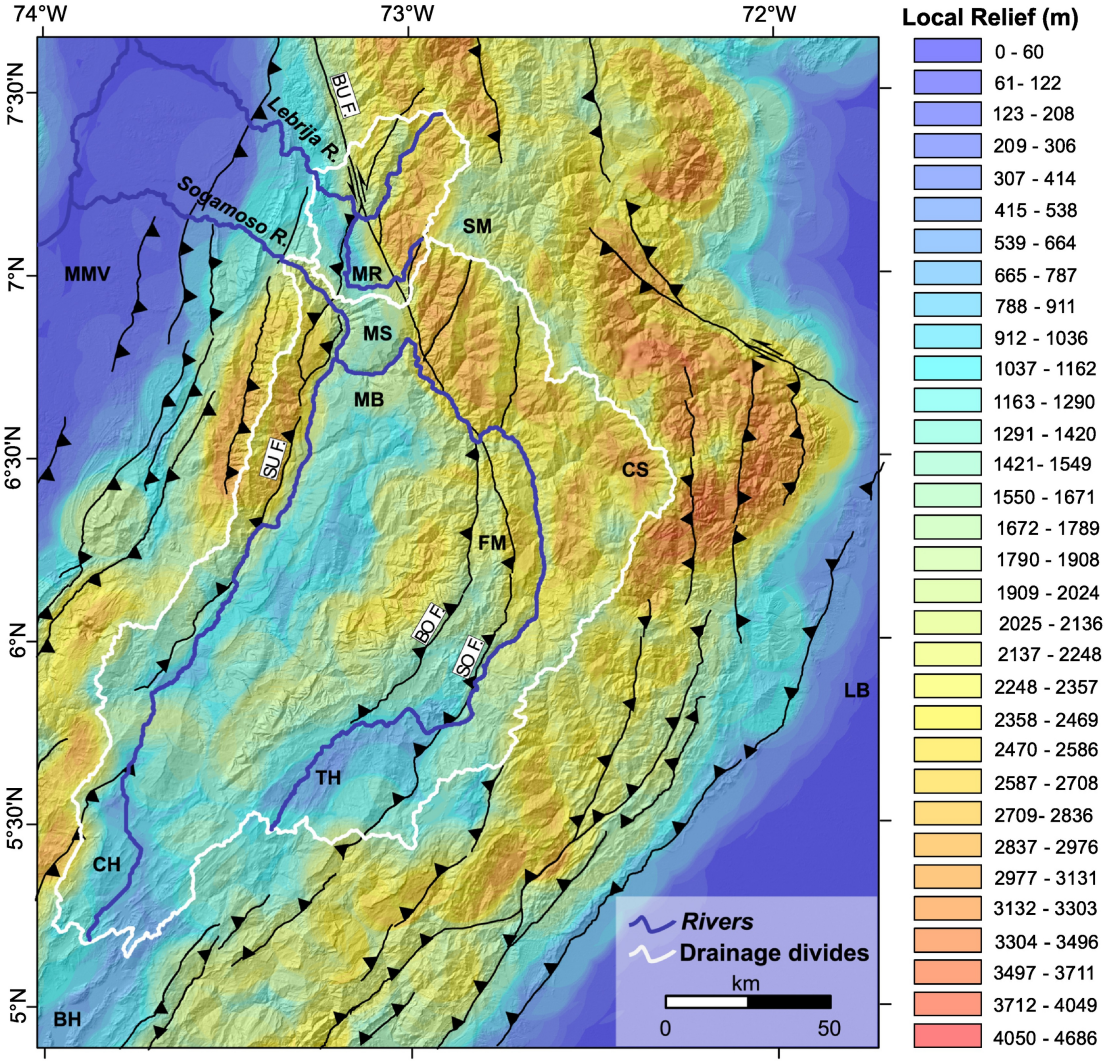
74°W
73°W
72°W
7°30'N
7°N
6°30'N
6°N
5°30'N
5°N
Local Relief (m)
0 - 60
61- 122
123 - 208
209 - 306
307 - 414
415 - 538
539 - 664
665 - 787
788 - 911
912 - 1036
1037 - 1162
1163 - 1290
1291 - 1420
1421- 1549
1550 - 1671
1672 - 1789
1790 - 1908
1909 - 2024
2025 - 2136
2137 - 2248
2248 - 2357
2358 - 2469
2470 - 2586
2587 - 2708
2709- 2836
2837 - 2976
2977 - 3131
3132 - 3303
3304 - 3496
3497 - 3711
3712 - 4049
4050 - 4686
Lebrija R.
Sogamoso R.
BU.F.
SU.F.
BO.F.
SO.F.
MMV
SM
MR
MS
MB
CS
FM
TH
CH
BH
LB
Rivers
Drainage divides
km
0
50

Figure 6

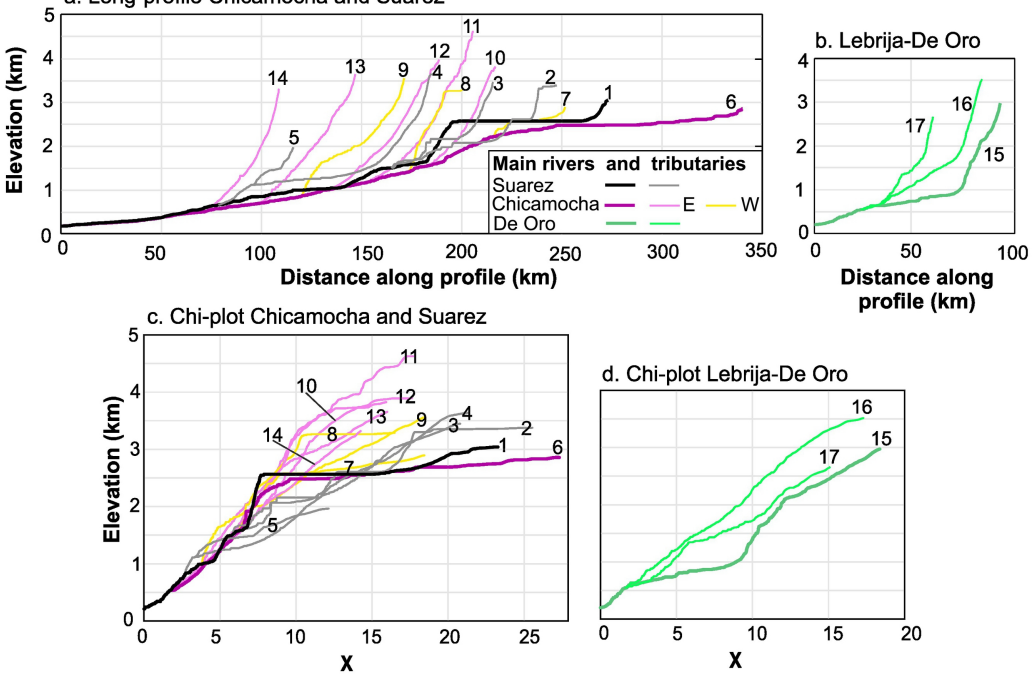
a. Long-profile Chicamocha and Suarez
Elevation (km)
Distance along profile (km)
Main rivers and tributaries
Suarez
Chicamocha
De Oro
E
W
b. Lebrija-De Oro
Distance along profile (km)
c. Chi-plot Chicamocha and Suarez
Elevation (km)
X
d. Chi-plot Lebrija-De Oro
X

Figure 7

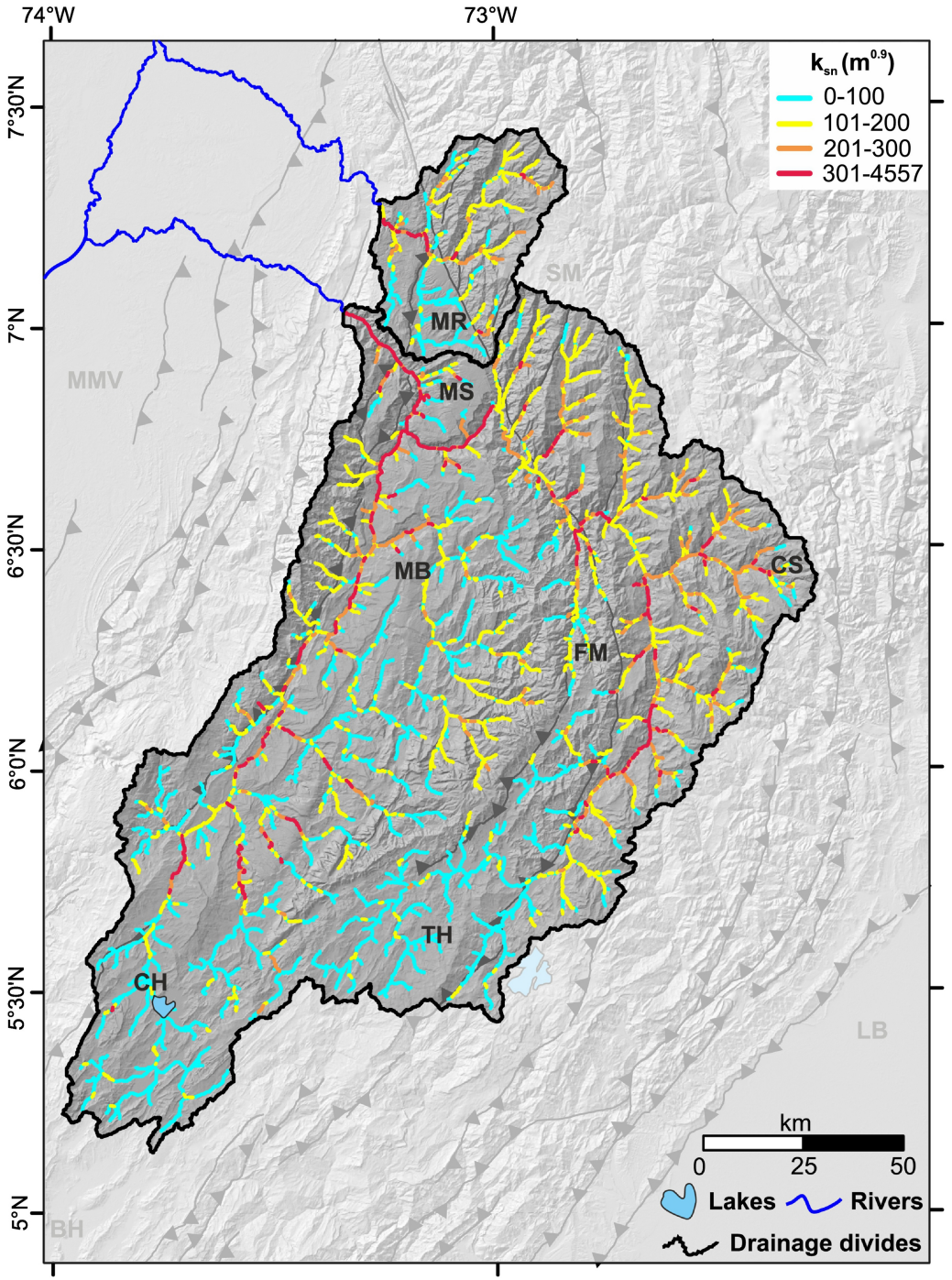
74°W
73°W
7°30'N
7°N
6°30'N
6°0'N
5°30'N
5°N
k_{sn} ($m^{0.9}$)
0-100
101-200
201-300
301-4557
SM
MR
MMV
MS
MB
CS
FM
TH
CH
LB
BH
km
0
25
50
Lakes
Rivers
Drainage divides

Figure 8

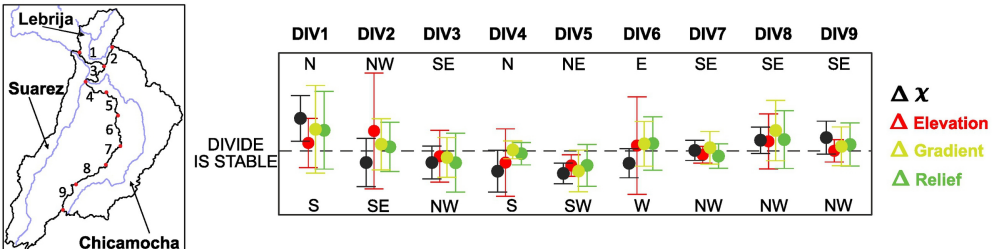
Lebrija
Suarez
Chicamocha
1
2
3
4
5
6
7
8
9
DIV1
DIV2
DIV3
DIV4
DIV5
DIV6
DIV7
DIV8
DIV9
N
NW
SE
N
NE
E
SE
SE
SE
DIVIDE
IS STABLE
S
SE
NW
S
SW
W
NW
NW
NW
Δ χ
Δ Elevation
Δ Gradient
Δ Relief

Figure 9

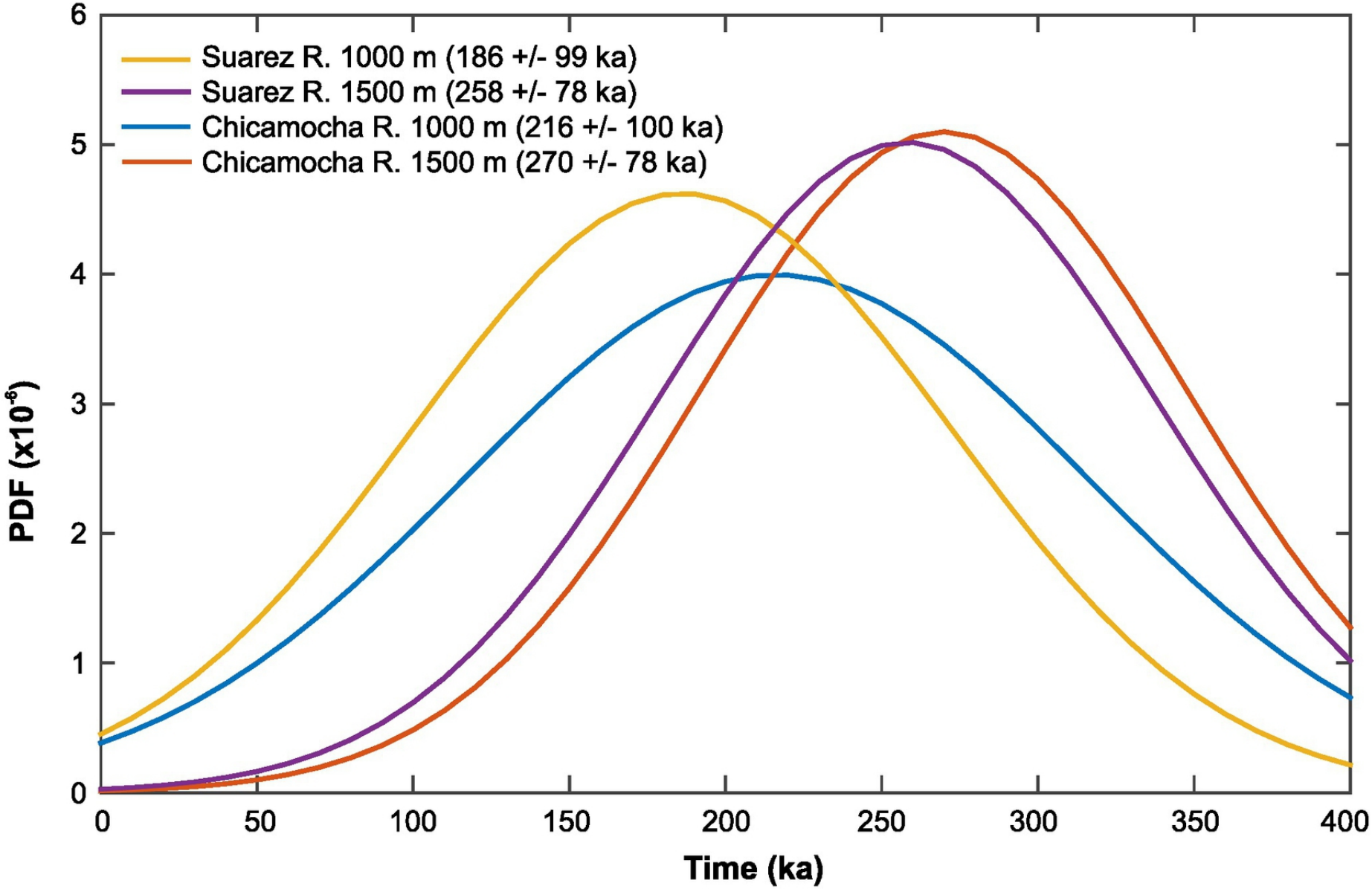
Suarez R. 1000 m (186 +/- 99 ka)
Suarez R. 1500 m (258 +/- 78 ka)
Chicamocha R. 1000 m (216 +/- 100 ka)
Chicamocha R. 1500 m (270 +/- 78 ka)
PDF (x10^-6)
Time (ka)
0
1
2
3
4
5
6
0
50
100
150
200
250
300
350
400

Figure 10

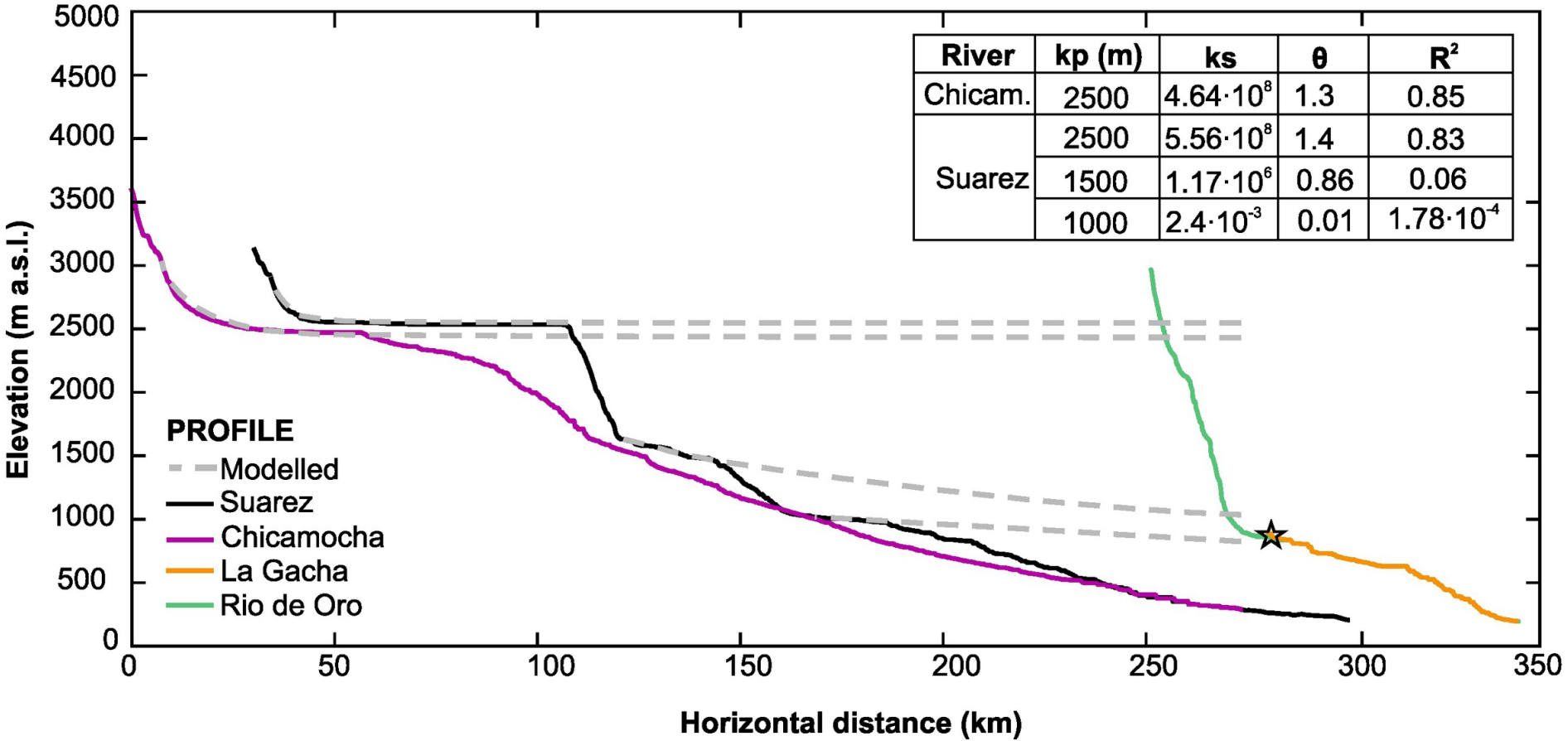
River | kp (m) | ks | θ | R²
Chicam. | 2500 | 4.64·10⁸ | 1.3 | 0.85
Suarez | 2500 | 5.56·10⁸ | 1.4 | 0.83
Suarez | 1500 | 1.17·10⁶ | 0.86 | 0.06
Suarez | 1000 | 2.4·10⁻³ | 0.01 | 1.78·10⁻⁴
PROFILE
Modelled
Suarez
Chicamocha
La Gacha
Rio de Oro
Elevation (m a.s.l.)
Horizontal distance (km)
0
500
1000
1500
2000
2500
3000
3500
4000
4500
5000
0
50
100
150
200
250
300
350

Figure 11

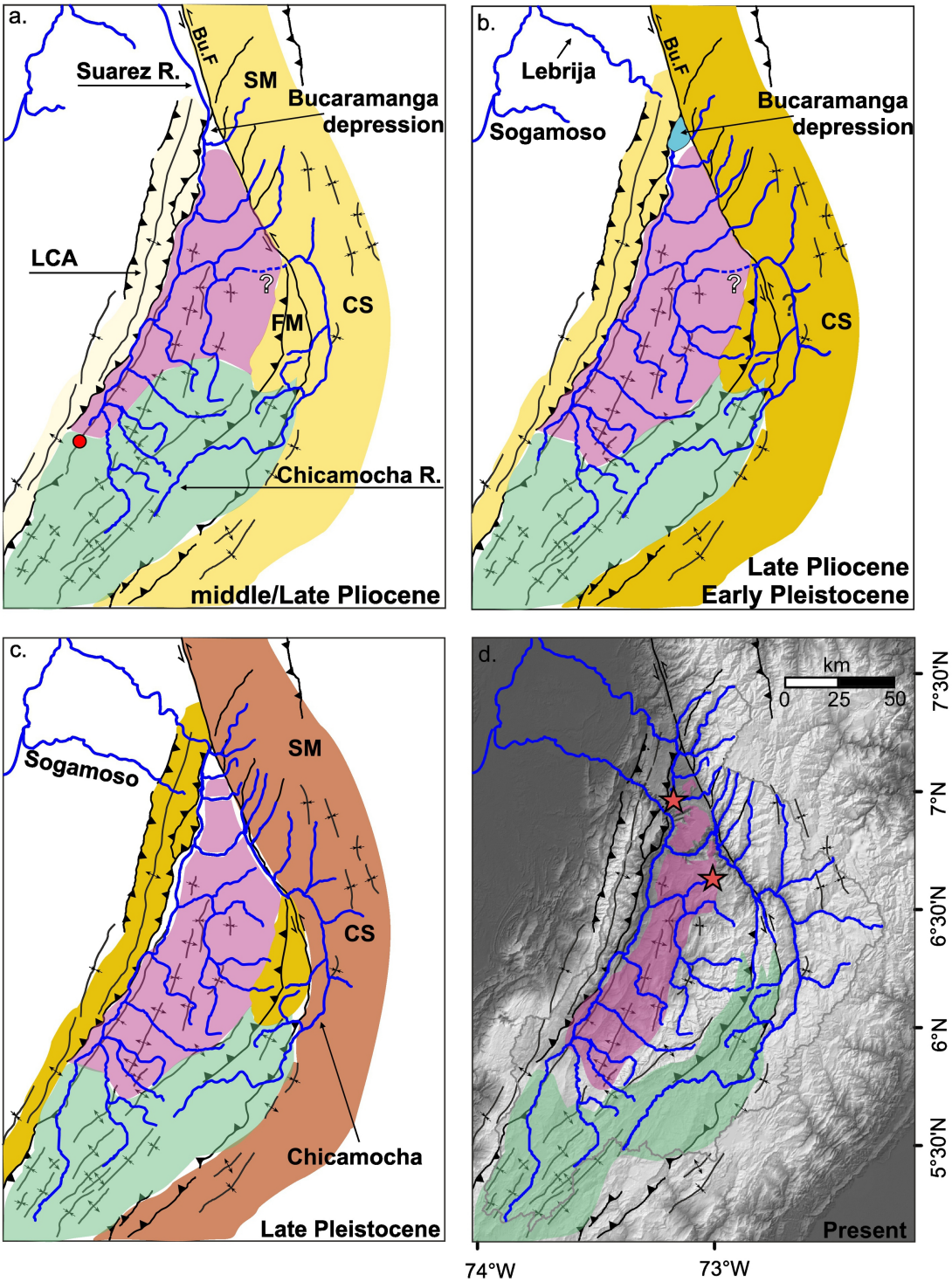
a.
Bu.F
Suarez R.
SM
Bucaramanga
depression
LCA
FM
CS
Chicamocha R.
middle/Late Pliocene
b.
Lebrija
Bu.F
Sogamoso
Bucaramanga
depression
CS
Late Pliocene
Early Pleistocene
c.
Sogamoso
SM
CS
Chicamocha
Late Pleistocene
d.
km
0
25
50
Present
74°W
73°W
7°30'N
7°N
6°30'N
6°N
5°30'N
Topography
Lower
Higher
Paleolandscapes
Upper (Highlands)
Lower (Mesas)
Morphologic features
windgap
damming landslides

Figure 12